NASA TECHNICAL NOTE

NASA TN D-3960

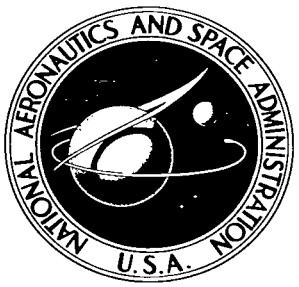

NASA TN D-3960

WIND-TUNNEL TESTS OF A SERIES OF PARACHUTES DESIGNED FOR CONTROLLABLE GLIDING FLIGHT

by James A. Weiberg and Kenneth W. Mort

Ames Research Center

Moffett Field, Calif.

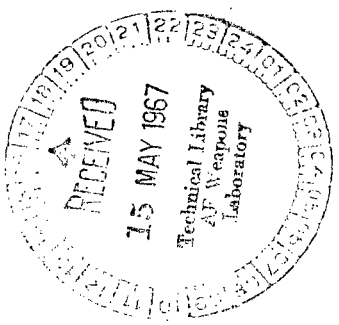

NATIONAL AERONAUTICS AND SPACE ADMINISTRATION • WASHINGTON, D. C. • MAY 1967

NASA TN D-3960

WIND-TUNNEL TESTS OF A SERIES OF PARACHUTES DESIGNED FOR CONTROLLABLE GLIDING FLIGHT

By James A. Weiberg and Kenneth W. Mort

Ames Research Center
Moffett Field, Calif.

NATIONAL AERONAUTICS AND SPACE ADMINISTRATION

For sale by the Clearinghouse for Federal Scientific and Technical Information
Springfield, Virginia 22151 – CFSTI price $3.00

WIND-TUNNEL TESTS OF A SERIES OF PARACHUTES DESIGNED FOR CONTROLLABLE GLIDING FLIGHT

By James A. Weiberg and Kenneth W. Mort

Ames Research Center

SUMMARY

It was found that the glide capability of parachutes was affected by the canopy configuration. The maximum lift-drag ratio achieved was approximately 2.1 and was attained by two parachutes, a rectangular canopy and a 3-lobe canopy. This performance was generally obtained with some loss in stability, particularly at low lift-drag ratios corresponding to nearly vertical descent. Limited results of an investigation of two reefed configurations are also presented.

INTRODUCTION

The characteristics desired of a recovery parachute are high maximum lift-to-drag ratio (L/D) with ability to control the glide angle from vertical descent (L/D = 0) to the maximum L/D. Research reported in reference 1 showed that the glide path of a parachute could be controlled by use of an extendable flap in one side of the canopy. The maximum glide path angle of these parachutes was limited by distortion and collapse of the leading edge of the canopy. Additional tests were made of parachute configurations designed to maintain canopy shape to higher glide angles and the results are presented in this report. The tests were conducted in the Ames 40- by 80-foot wind tunnel.

NOTATION

b reference span of rectangular parachutes, ft

C_D drag coefficient, $\frac{\text{drag}}{qS_o}$

C_L lift coefficient, $\frac{\text{lift}}{qS_o}$

C_R resultant force coefficient, $\sqrt{C_L^2 + C_D^2}$

D_o nominal diameter of uninflated parachute, ft

h suspension line length, ft

$\frac{L}{D}$ lift-drag ratio

q free-stream dynamic pressure, psf

S_o nominal uninflated parachute area $\frac{\pi D_o^2}{4}$, or reference area, sq ft

V free-stream velocity, fps

Δl_i internal control line extension (see figs. 2(c) and 2(f))

Δl_c control line extension, ft

MODEL AND APPARATUS

Parachutes

The parachutes primarily have solid canopies. Single- and multiple-lobe canopies and clusters of single canopies were tested. Photographs of the parachutes in the tunnel are shown in figure 1. The geometry of the parachutes is given in figure 2. Configurations 1 to 6 (figs. 2(a) to 2(d)) are single circular canopies. The three devices investigated to prevent canopy leading-edge collapse are shown in figure 2(e) and consist of (1) a curved aluminum tube inserted into the leading edge of the canopy, (2) a torus inflated to 0.8 psi with nitrogen and attached to the skirt of the canopy, and (3) triangularly shaped struts attached to the leading edge of the canopy at the suspension lines. Configurations 7 and 8 (fig. 2(f)) are multiple-lobe canopies and represent a cluster of three parachutes in a single canopy. Configurations 9, 10, and 11 (figs. 2(g) to 2(i)) are rectangular canopies. The sailcloth porosity (cfm/sq ft at a differential pressure of 0.5 inch of water) was 2 for configurations 1 to 8 and 0.5 for configurations 9 to 11.

The circular and multiple-lobe canopies (configurations 1 to 8) had controllable trailing-edge flaps. Configurations 5 and 7 also had controllable internal suspension lines (see figs. 2(c) and 2(f)). The rectangular canopies (configurations 9, 10, and 11) had control lines attached as shown in figures 2(g), (h), and (i).

Parachute configurations 1 to 8 were designed and fabricated by the Ventura Division of Northrop Corporation. Configurations 9, 10, and 11 were designed and fabricated by Barish Associates, Inc.

Control Mechanism and Tunnel Mounting

The mechanism which operated the control lines is shown in figure 3, and is similar to the one described in reference 1.

The parachutes were mounted in the tunnel either on one of the conventional model support struts (fig. 4(a)) or on a short strut (fig. 4(b)). On the conventional strut, the control mechanism was attached rigidly to the strut and the parachute was "flown" in an approximately horizontal plane near the center of the tunnel. On the short strut, the control mechanism was mounted on a gimbal arrangement which allowed the mechanism to pivot about a horizontal axis so that the parachute was "flown" in a vertical plane.

Tests and Corrections

The parachutes were tested for a range of control settings and tunnel velocities. Tests of configurations 1 to 8 began with a low stable flap setting. The flap extension was then increased until the parachute oscillated. Tests of configurations 9 to 11 began at maximum L/D, which occurred just prior to the collapse of the leading edge. The control lines were then retracted until the canopy oscillated. The data presented in the figures represent the maximum range of control settings with which the parachutes could be flown without oscillating violently.

Parachutes 5 and 7 were also tested in several reefed conditions. The parachutes were reefed at the skirt for several skirt diameters, and the drag was then determined for each diameter.

Lift and drag were measured by the regular wind-tunnel balance system. The drag data have been corrected for the drag of the supports. No corrections have been applied to the data for blockage or the effects of the tunnel walls because these corrections are estimated to be less than 1 percent.

RESULTS AND DISCUSSION

Glide Performance

The aerodynamic characteristics of various single canopy configurations are shown in figure 5 by presenting C_L, C_D, and L/D as functions of control line setting. Results are shown for various forward velocities, canopy sizes, and suspension line lengths. If not indicated, the parachutes were flown in a vertical plane. Three of the configurations were flown both vertically and horizontally to evaluate the test technique. Figures 5(a), (b), and (c) indicate some differences in the L/D depending on whether the

parachute was flown in a horizontal or vertical plane. However, these differences are within the repeatability of the data on a given parachute as shown in figures 5(b) and (c).

It is apparent from the results of figure 5 that of the single canopy configurations investigated, the rectangular canopies (configurations 9 to 11) achieved the highest values of L/D. The maximum value was about 2.1. The maximum L/D achieved by all of the configurations investigated was limited by collapse of the canopy leading edge. To delay or prevent this collapse the effects of modifications to the shape of the canopy leading edge and the effects of leading-edge support devices (see figs. 2(a) and 2(e)) on the aerodynamic characteristics of the basic single circular canopy (configuration 4) were investigated. The results are shown in figures 6 and 7. It can be inferred from these results that reshaping the leading edge or employing stiffening devices generally delayed collapse of the leading edge of the canopy. The inflated torus was the most effective device; it increased the L/D from about 1.1 to about 1.9 and, hence, appears to be a promising method of increasing the L/D capability of gliding parachutes.

Data from clusters of three parachutes and single canopy shapes resembling clusters (fig. 2(f)) are presented in figures 8 and 9. The three-lobe canopy (configuration 7) achieved a maximum L/D of 2.1.

Although the maximum L/D capability of the parachutes could be increased by varying canopy shape or adding leading-edge support devices (figs. 5 through 9), it was not possible to achieve zero L/D corresponding to a vertical descent. At control settings intended to produce low L/D, the parachutes oscillated violently in pitch and yaw. Analysis of the data in reference 2 indicated that parachute oscillations are primarily due to a static instability resulting from insufficient canopy porosity. The porosity of the sailcloth was essentially zero and there was very little geometric porosity.

Effect of Geometric Porosity

The geometric porosity of the three-lobe canopy (fig. 2(f)) was varied by increasing the vent opening on each lobe. The parachute with a porosity of 6 percent achieved a minimum L/D of 0.3. At low L/D the parachute was operating near or in the wake of the support strut; hence its stability could be affected by this wake. Maximum L/D and the corresponding resultant force coefficient decreased with increasing porosity (figs. 10 and 11). Similar porosity studies were not performed on the other configurations investigated. However, these results are considered to be generally applicable for gliding parachutes employing sailcloth which is essentially nonporous.

Drag in Reefed Configuration

In addition to glide performance, the drag of parachutes 5 and 7 with the skirt reefed to various diameters was determined. The effect of reefed diameter on parachute drag is shown in figure 12. With the parachutes reefed at the diameters investigated (up to 60 percent D_o for configuration 5) the parachute oscillations were reasonably small and the parachute did not produce a significant amount of lift.

CONCLUDING REMARKS

Maximum L/D was limited by collapse of the canopy leading edge and minimum L/D was limited by the uncontrollable oscillation of the canopy. When the canopy leading edge was supported with an inflatable torus, the collapse was delayed and maximum L/D achieved was about 1.9. This was nearly double the value without the torus. The glide capability of the parachutes investigated was affected by canopy configuration. Three-lobe and rectangular shaped canopies attained the highest L/D, about 2.1. Generally, the canopies investigated had essentially zero porosity which is necessary for high maximum L/D. The use of centrally located geometric porosity reduced the maximum L/D but greatly increased the range of L/D which was not accompanied by oscillation of the canopy.

Ames Research Center
National Aeronautics and Space Administration
Moffett Field, Calif., Jan. 31, 1967
124-07-03-07-00-21

REFERENCES

1. Gamse, Berl; and Yaggy, Paul F.: Wind-Tunnel Tests of a Series of 18-Foot-Diameter Parachutes With Extendable Flaps. NASA TN D-1334, 1962.

2. Heinrich, Helmut G.; and Haak, Eugene L.: Stability and Drag of Parachutes With Varying Effective Porosity. ASD-TDR-62-100, Sept. 1962.

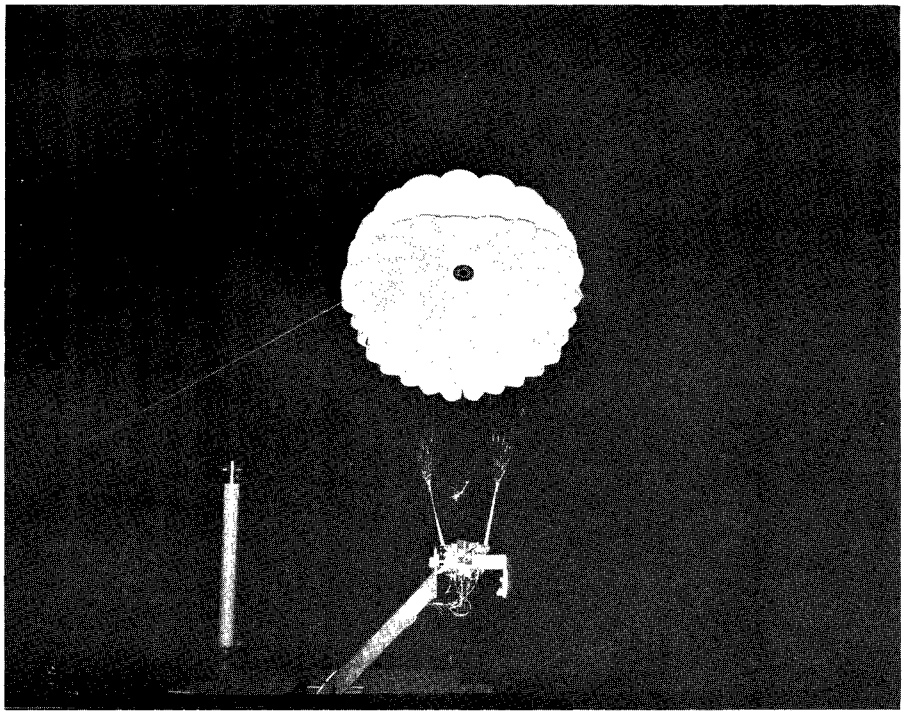

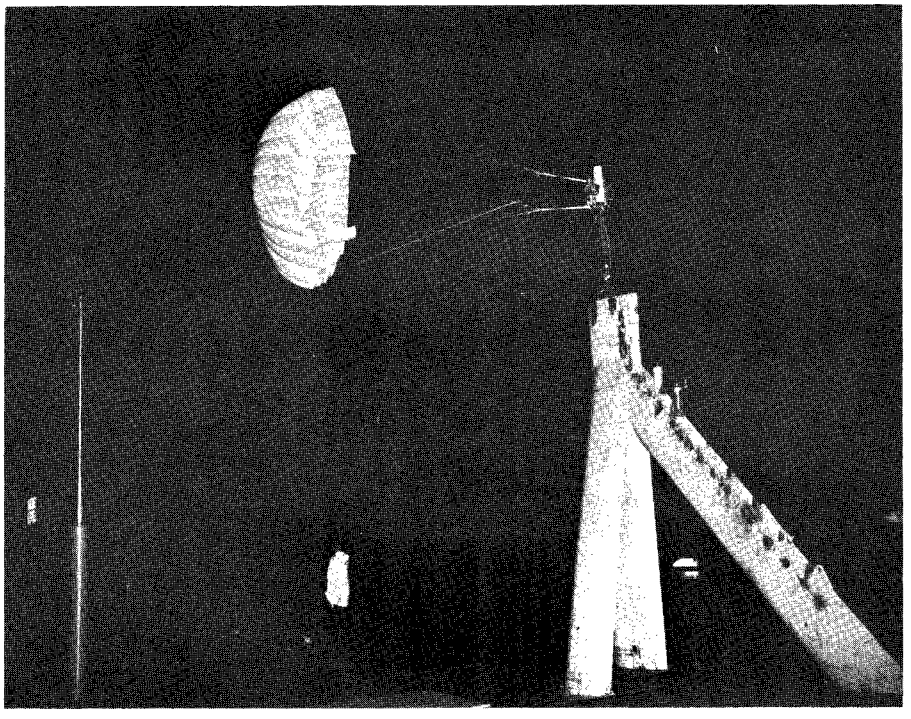

(a) Configuration 1.

Figure 1.- The parachutes mounted in the tunnel.

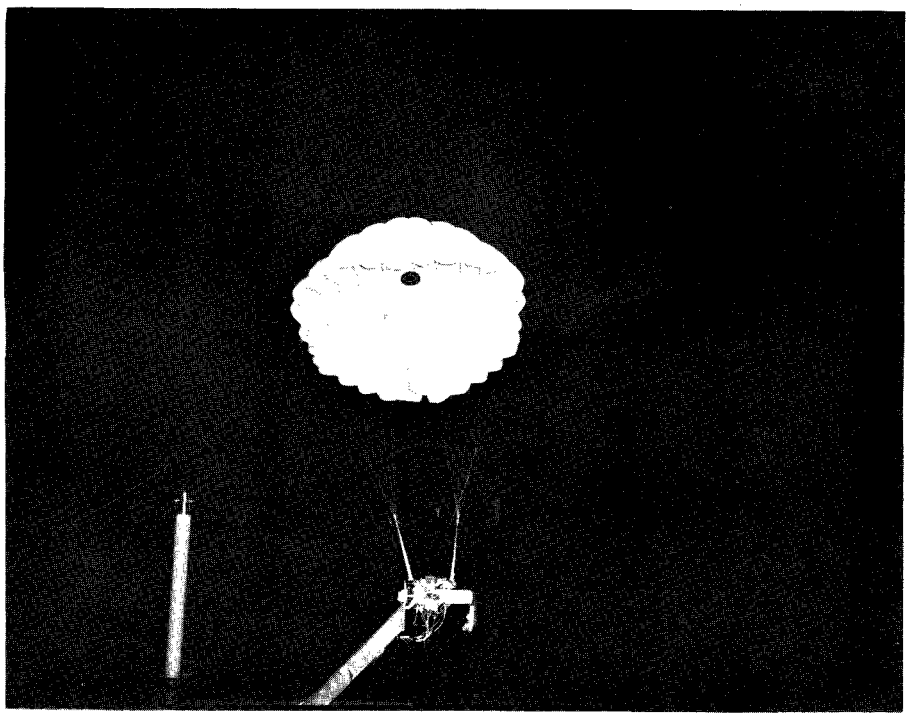

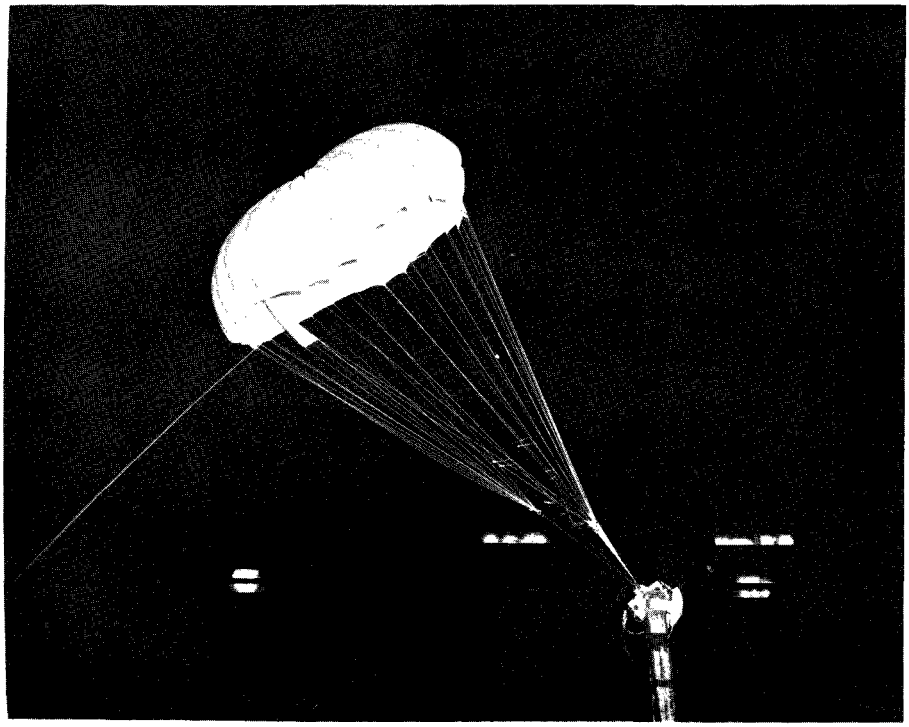

(b) Configuration 2.

Figure 1.- Continued.

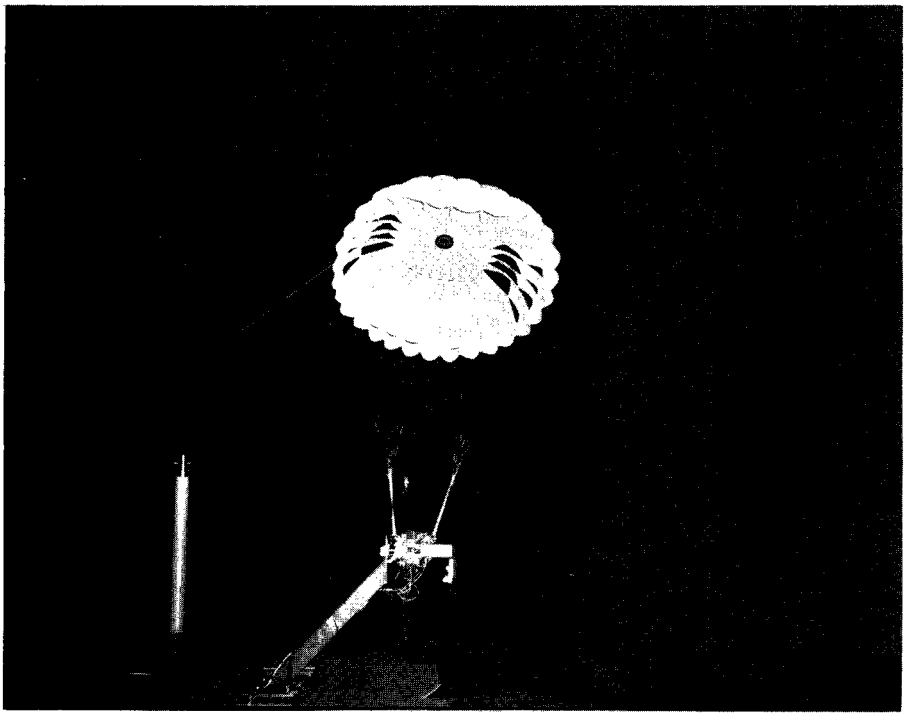

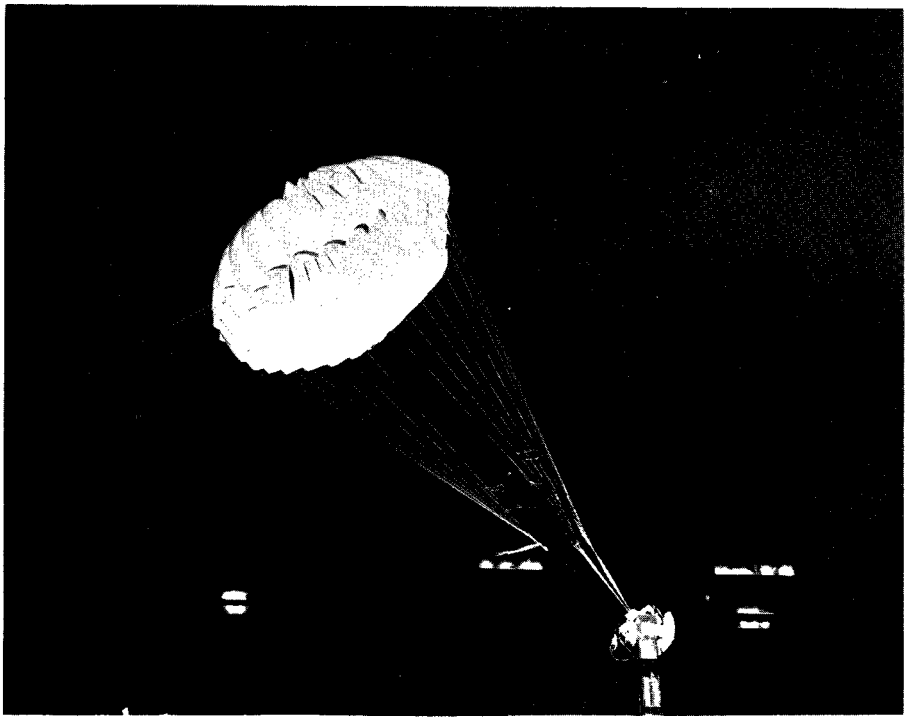

(c) Configuration 3.

Figure 1.- Continued.

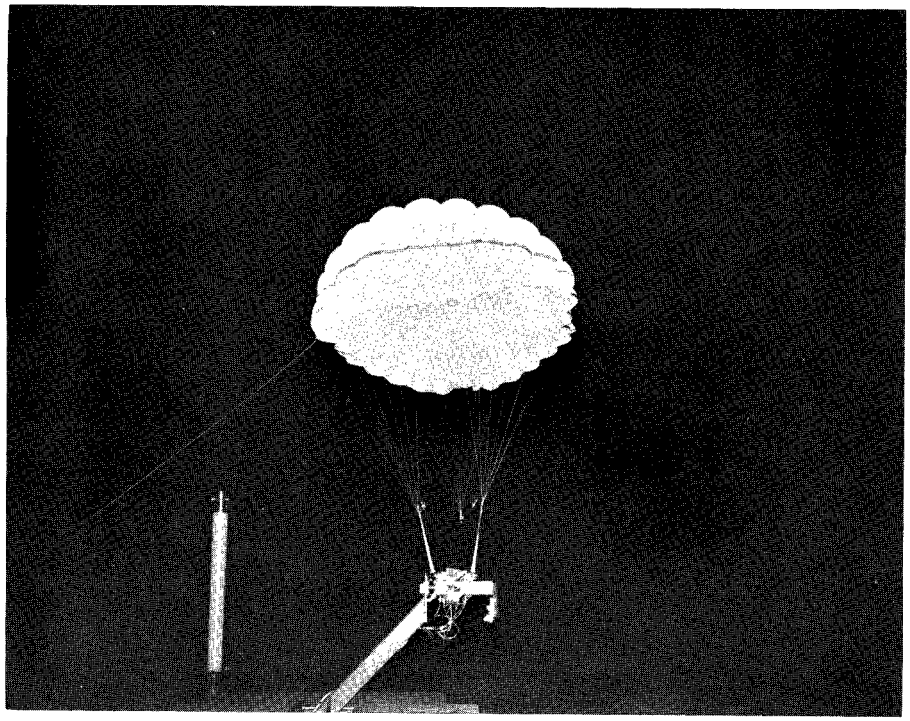

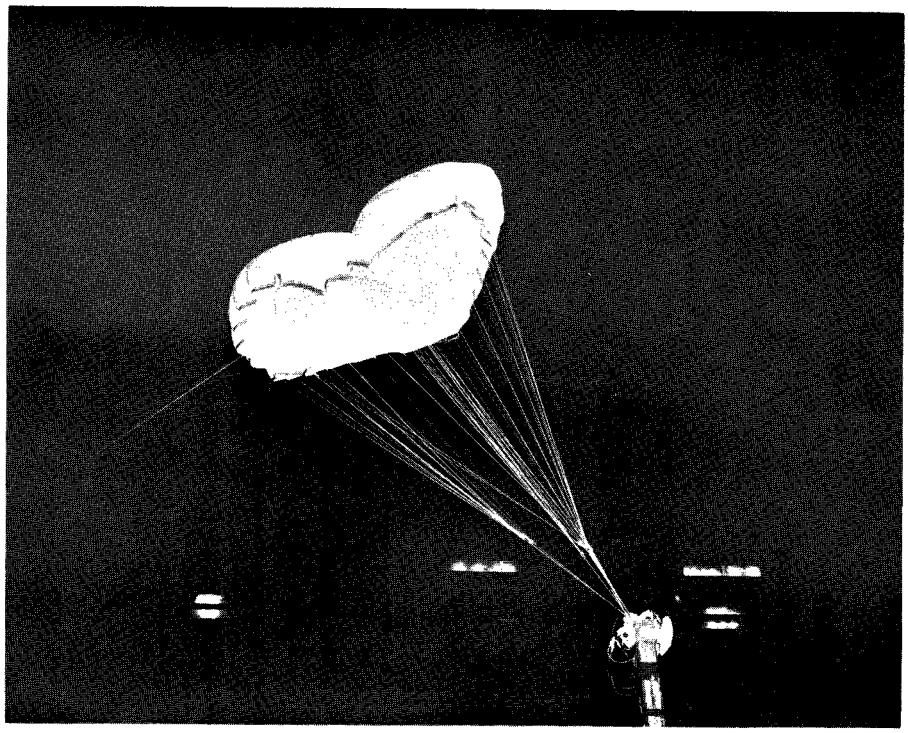

(d) Configuration 5.

Figure 1.- Continued.

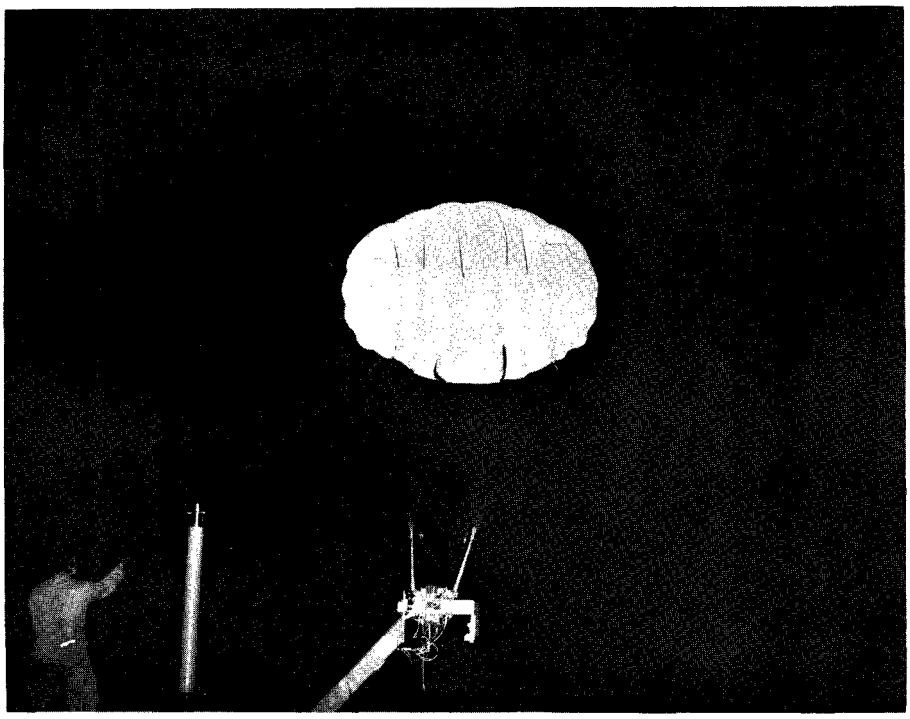

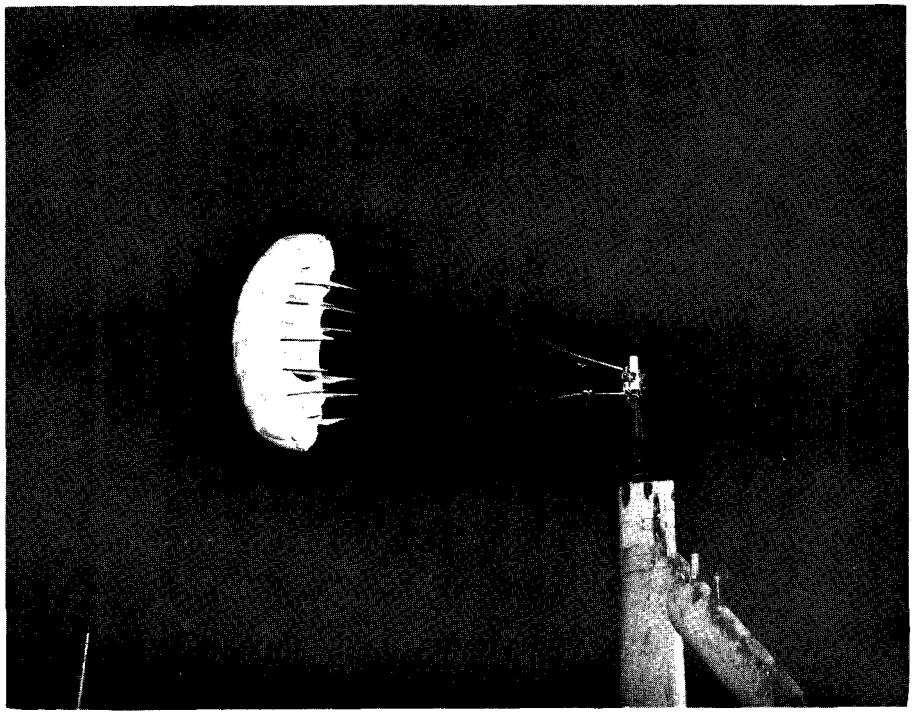

(e) Configuration 6.

Figure 1.- Continued.

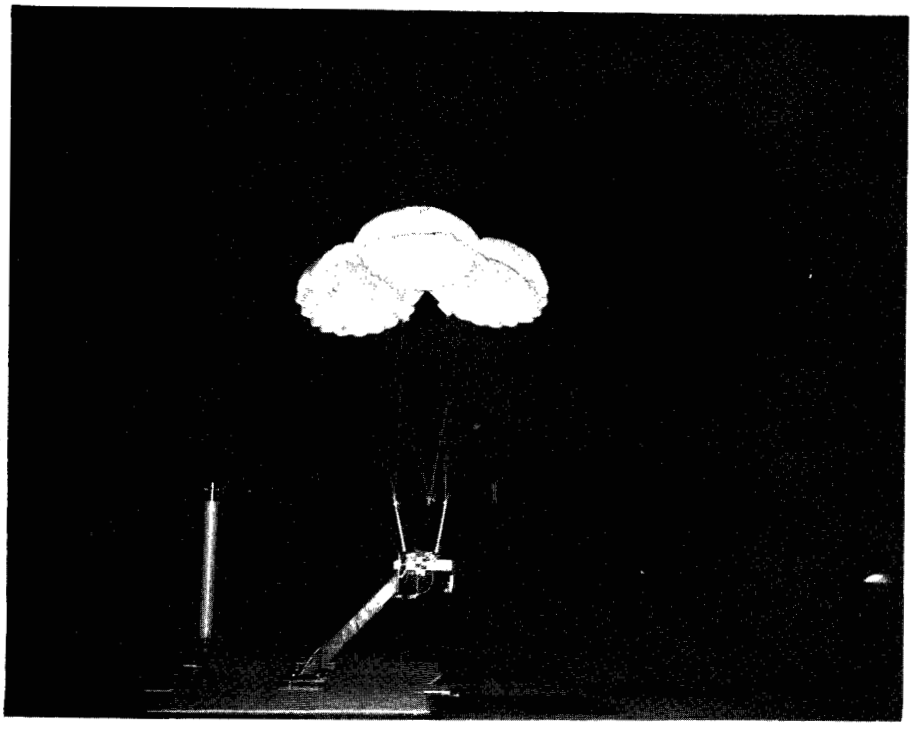

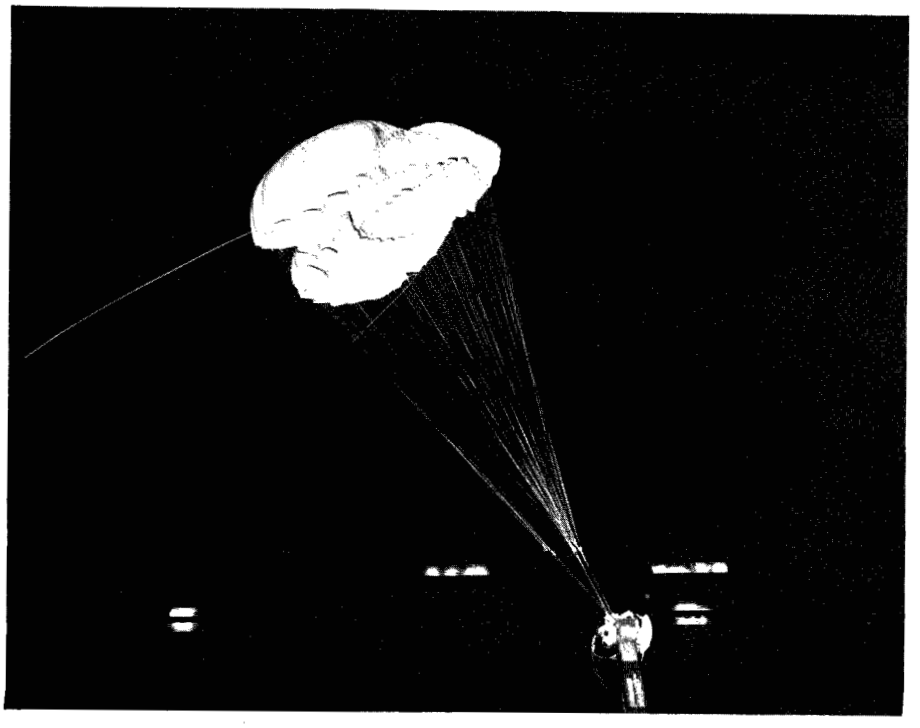

(f) Configuration 7.

Figure 1.- Continued.

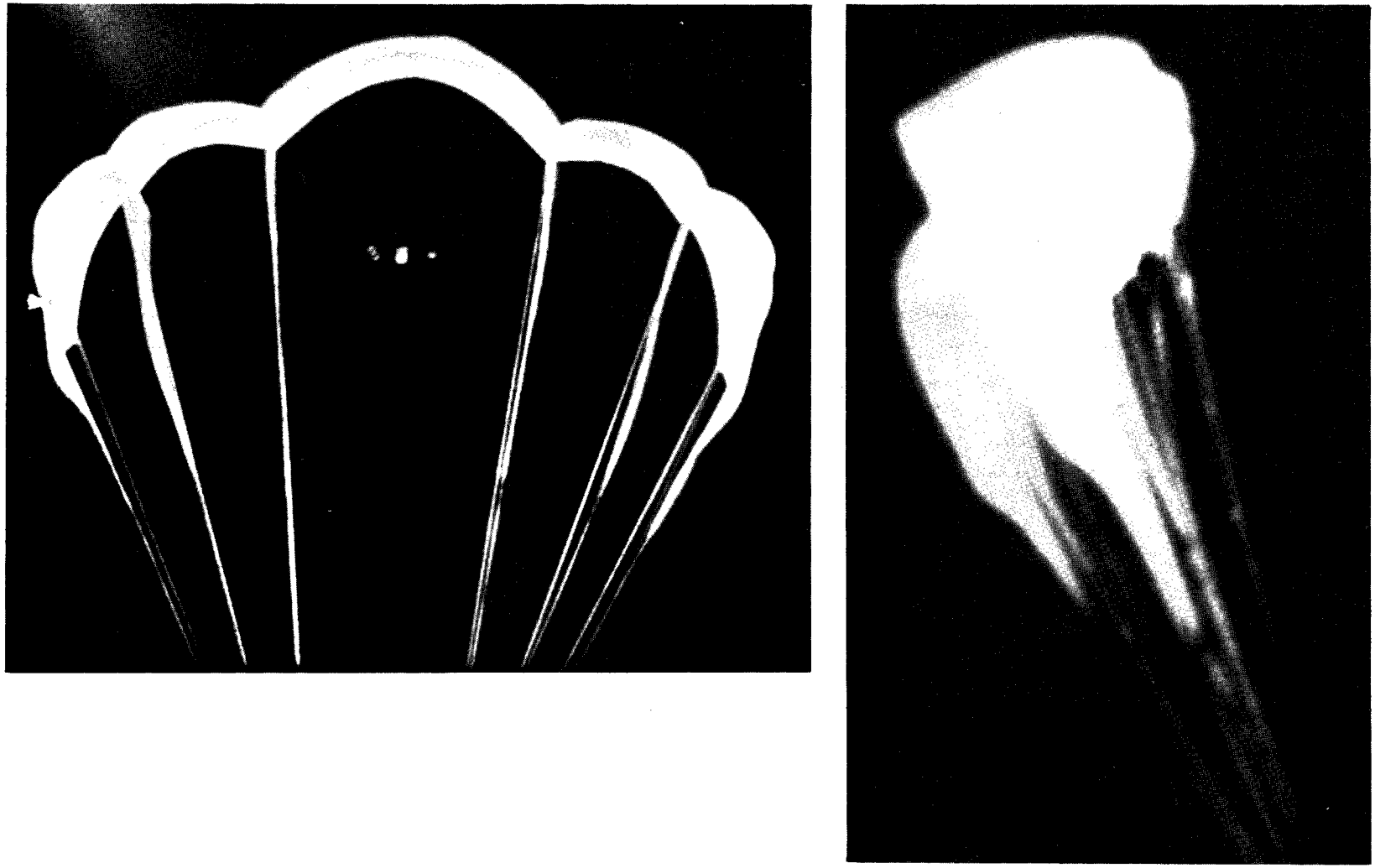

(g) Configuration 9.

Figure 1.- Continued.

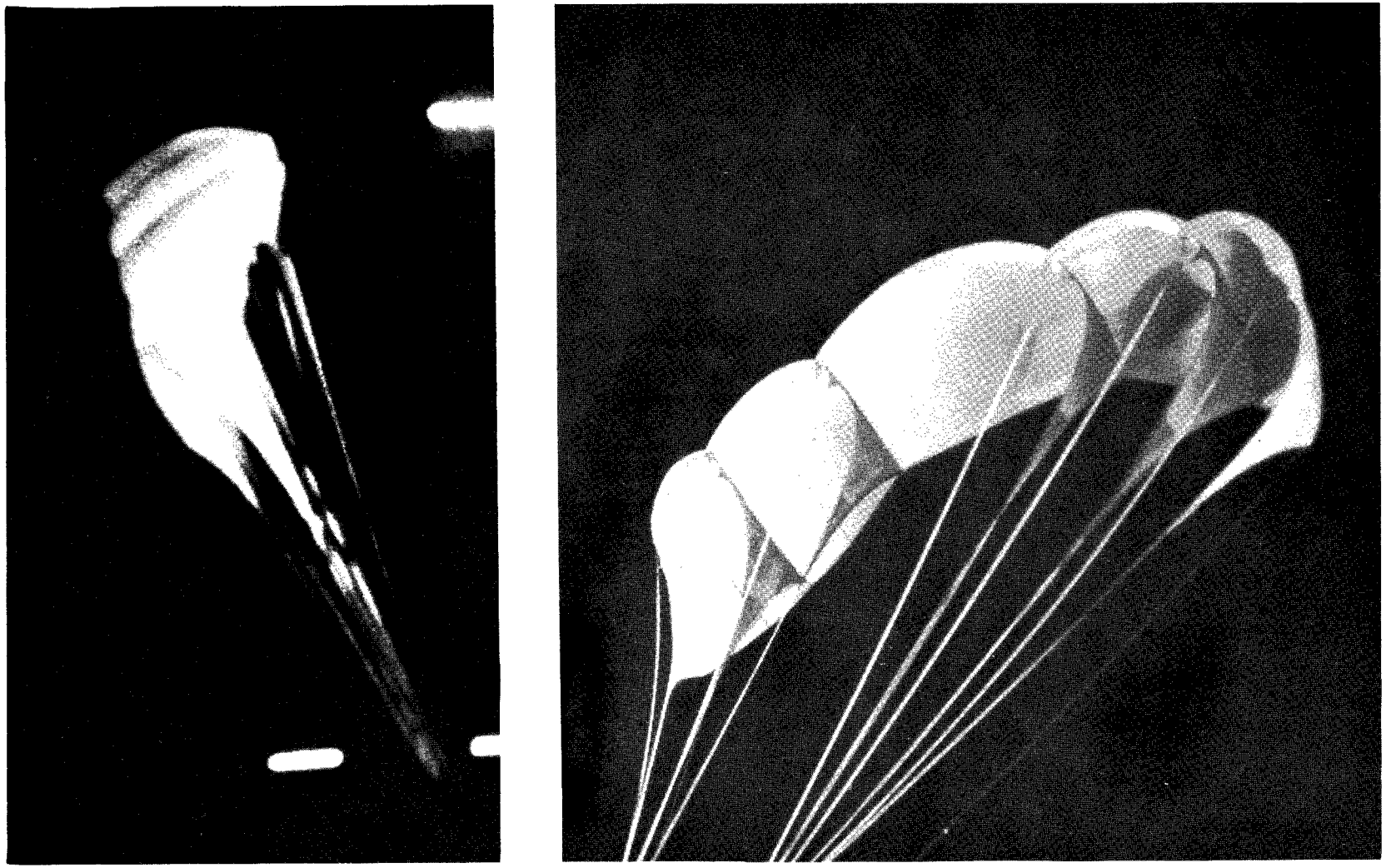

(h) Configuration 10.

Figure 1.- Continued.

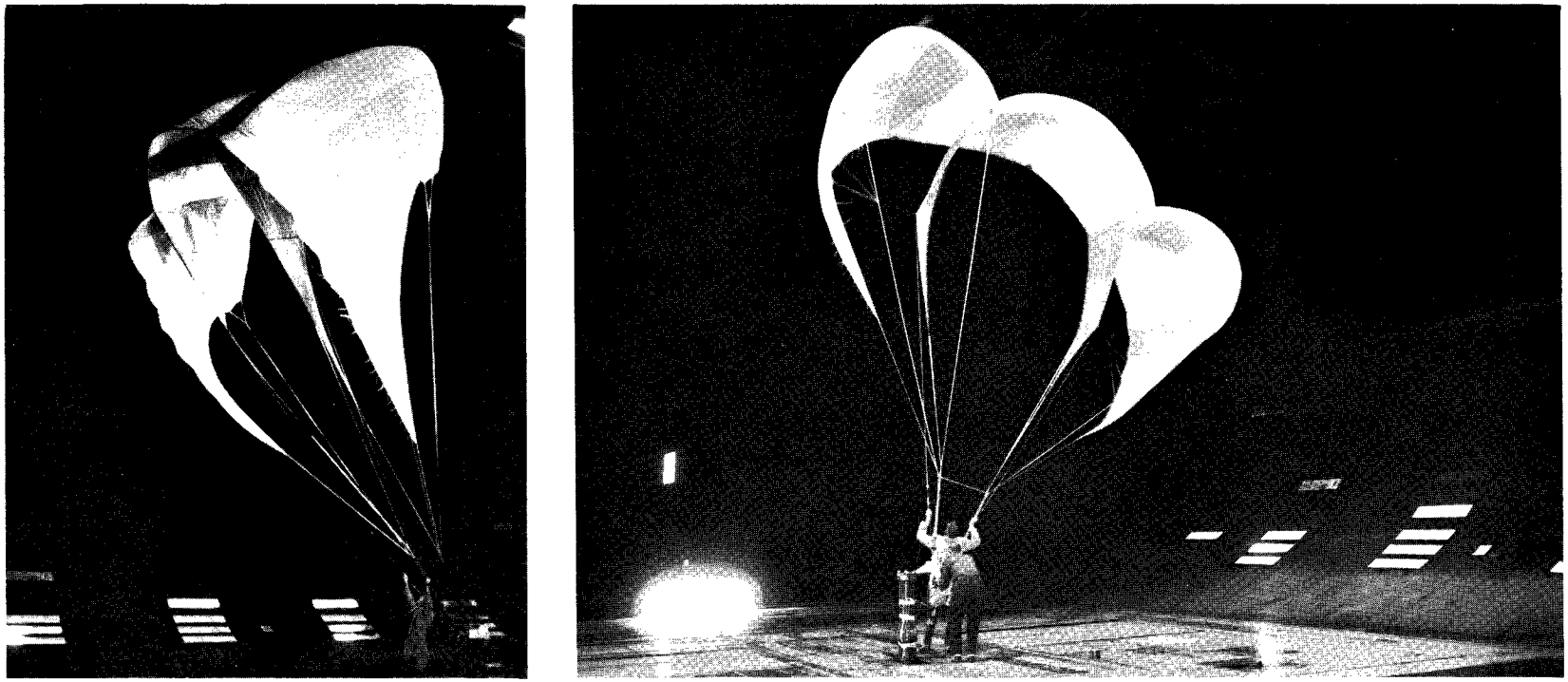

(i) Configuration 11.

Figure 1.- Concluded.

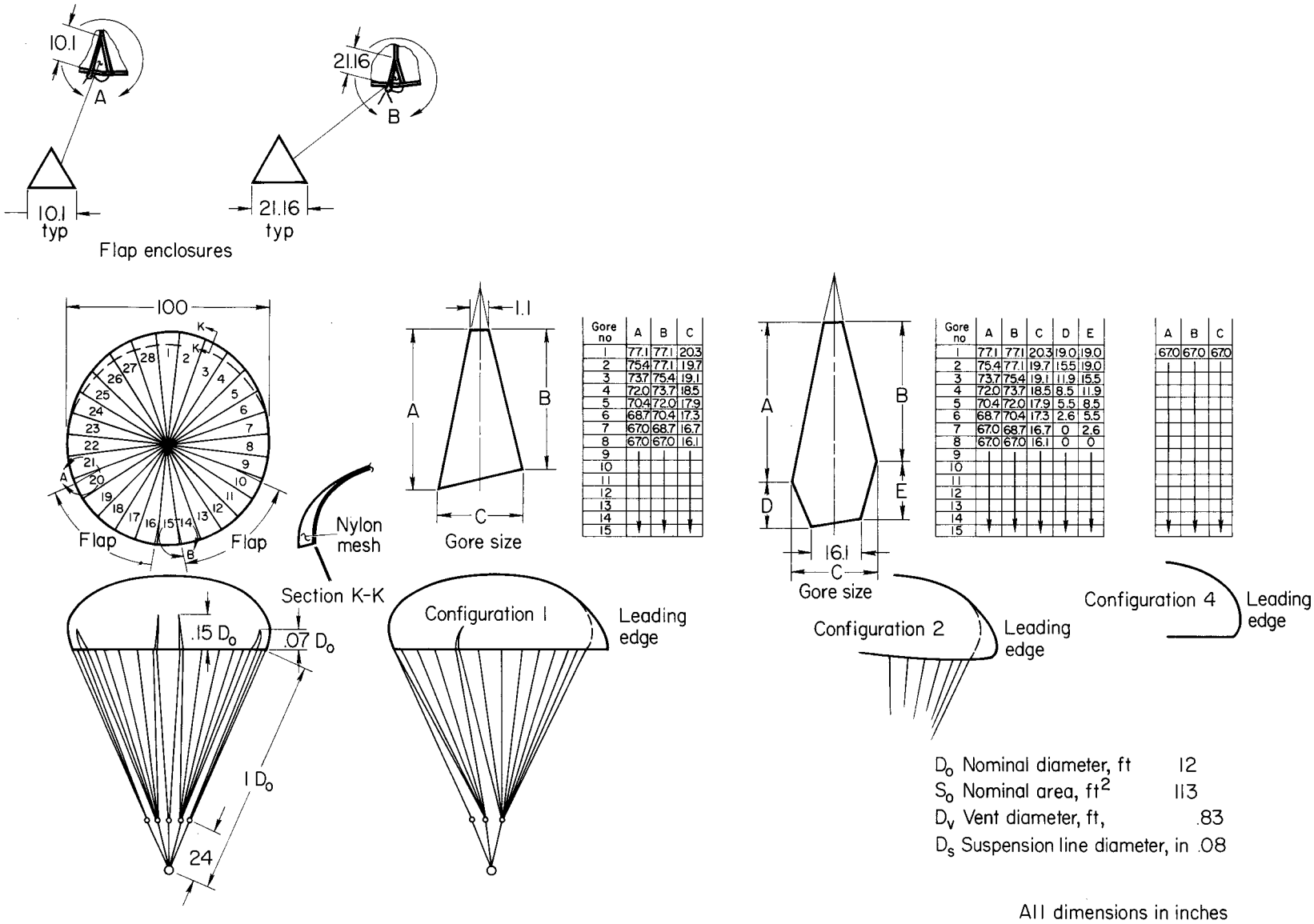

(a) Configurations 1, 2, and 4.

Figure 2.- Geometry of the parachutes.

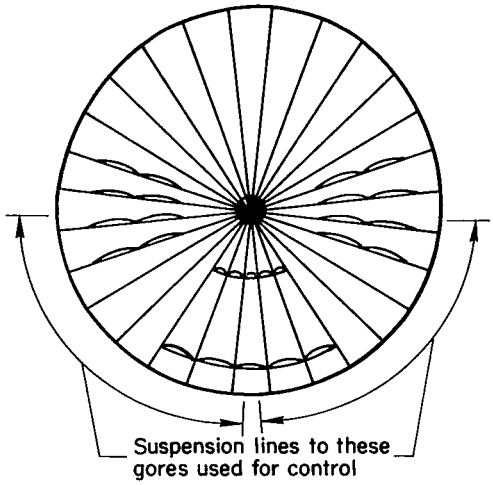

Same basic canopy as configuration I except for the addition of the louvers, as shown, and the absence of flaps

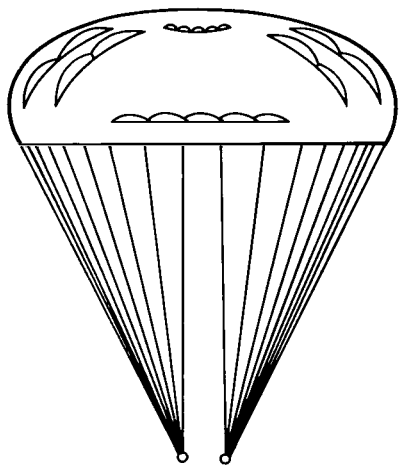

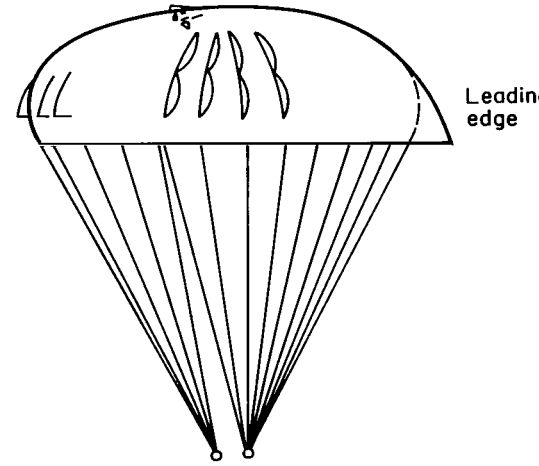

(b) Configuration 3.

Figure 2.- Continued.

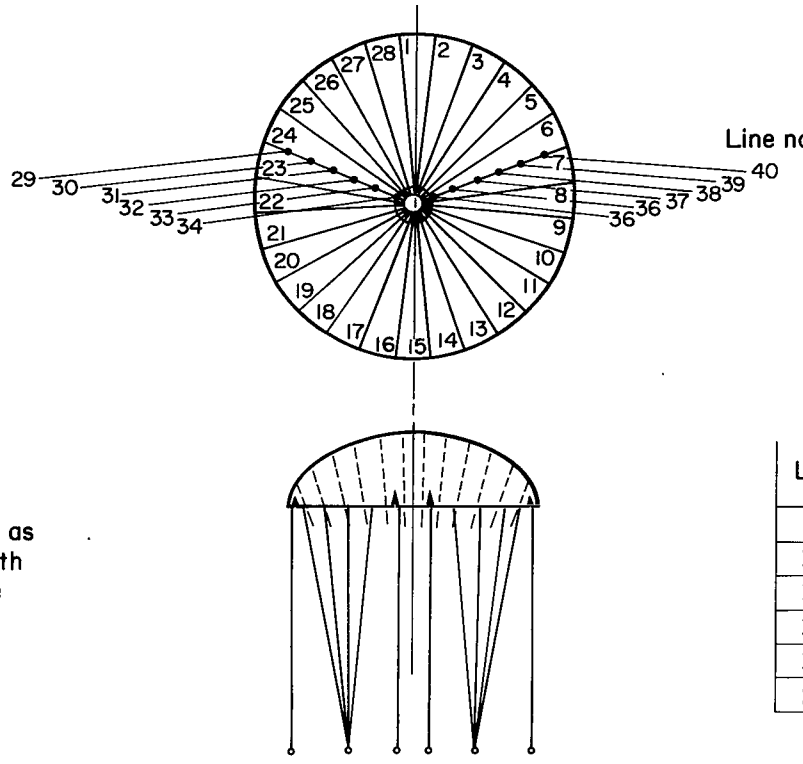

Same basic shape as configuration 2 with the addition of the center lines

Line no	Length $\frac{}{D_o}$
34, 35	.944
33, 36	.939
32, 37	.929
31, 38	.914
30, 39	.897
29, 40	.872

	Line location
	Lines 2 through 9 and 15 on rear center gore to one link plus line 29
	Lines 22 through 1 and 16 on rear center gore to one link plus line 40
These lines grouped together for Δl_c control	Flap lines 11 through 14 one link
	Flap lines 17 through 20 one link
	Flap lines 10, 15, 16 and 21 snap link
These lines grouped together for Δl_i control	Lines 30, 31, 38, and 39 one link
	Lines 32, 33, 34, 35, 36 and 37 one link

(c) Configuration 5.

Figure 2.- Continued.

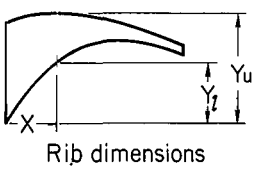

Rib dimensions

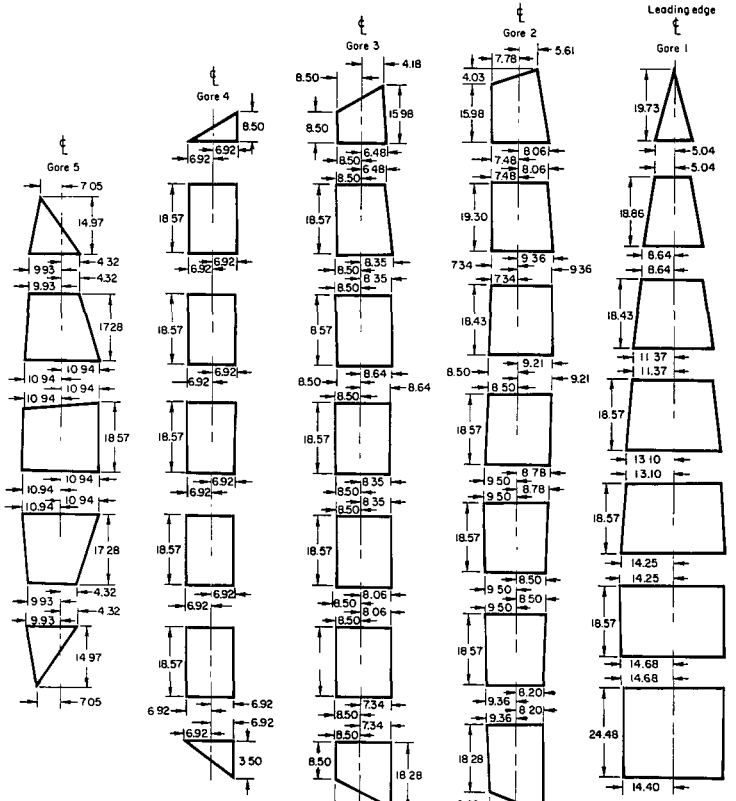

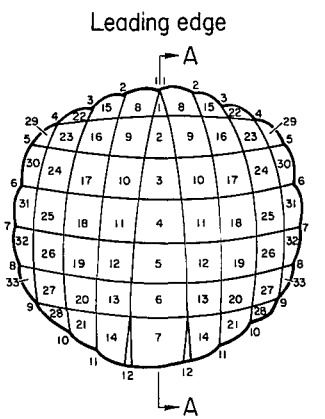

Trailing edge

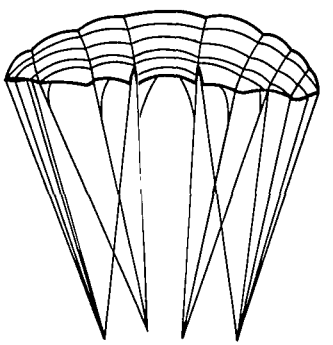

X	Leading edge						Trailing edge					
	Rib 1		2		3		1		2		3	
	Yu	Yl	Yu	Yl	Yu	Yl	Yu	Yl	Yu	Yl	Yu	Yl
0	35 14	0	29.66	0	24 91	0	39 16	0	33.00	0	27 85	0
7.20	35.42	10.80	30.24	9 74	25.34	9 79	3801	10.80	32 23	9 74	2732	979
14 40	34.96	18.28	30.09	17.28	25.34	15 30	36 14	18.28	31 10	17 28	26 48	15.30
21.60	33 54	22 17	29.23	20.16	24.91	18.14	33 98	22 17	29 44	20 16	25 28	18 14
28.80	31 25	23.76	2736	20.88	23 76	18 86	31 25	23.76	27 36	20.88	23 85	18 86
36.00	28.47	24 33	24.91	20 89	22 25	18 85	28 47	24 33	24 91	20 89	22 25	18.85
43.20	25.32	22.90	22.10	19.44	20.28	17 80	25.32	22.90	22.10	19.44	20 28	17 80
50 40	21 89	20 02	18.70	16.70	17 82	15.85	21 89	20 02	18 70	16 70	17 82	15 85
57.60	17 95	16.27	14.97	13 39	15 12	13.39	17 95	16 27	14 97	13 39	15 12	13.39
64.80	13.10	11 52	11 23	9 86			13.10	11 52	11 23	9.86		

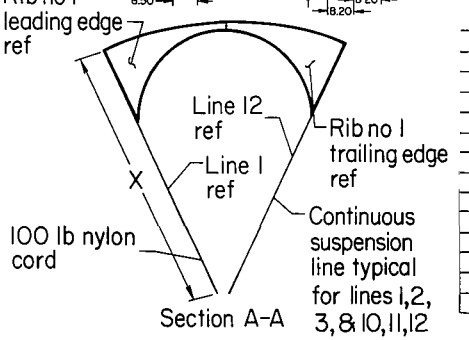

Suspension line data	
Line no	X/D_0
1	1 125
2	1 125
3	1 100
4	1 075
5	1 070
6	1 044
7	1.044
8	1 038
9	1 050
10	1 075
11	1.100
12	1.122

Nominal diameter, ft 12
Nominal area, ft^2 113
Suspension line diam, in. .08

All dimensions in inches

(d) Configuration 6.

Figure 2.- Continued.

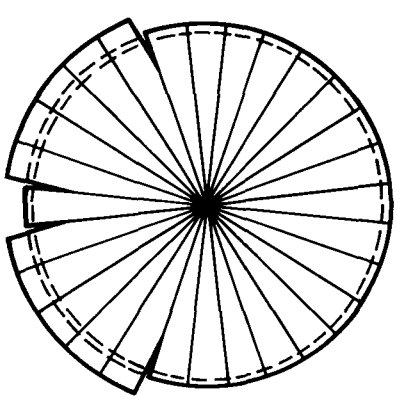

Configuration 4 with 6 inch inflatable torus

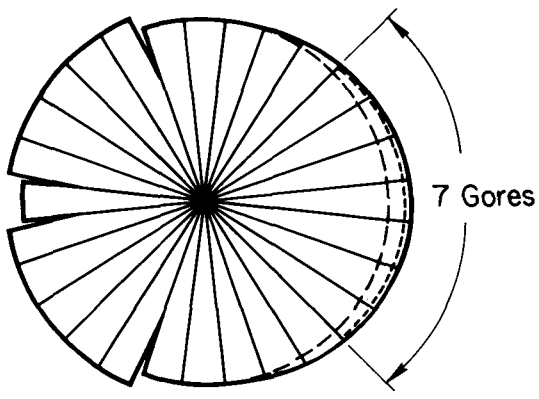

Configuration 1 with 1 1/4 inch aluminum tube leading edge stiffener

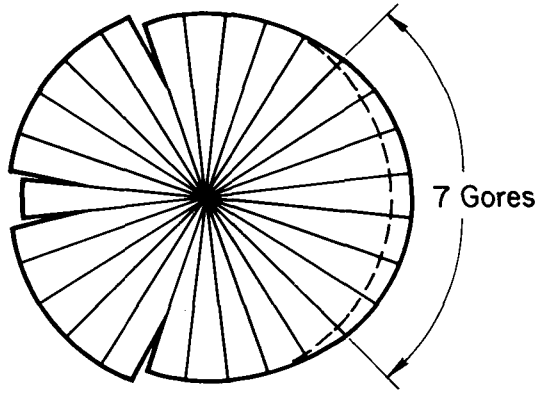

Configuration 1 with triangular leading edge stiffeners fabricated from 1/4 inch aluminum tubing

(e) Leading-edge stiffeners.

Figure 2.- Continued.

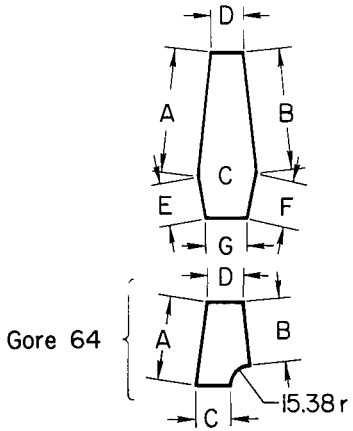

Gore no	A	B	C	D	E	F	G
1	38.50	38.50	11.20	1.25	11.00	11.00	11.36
2	38.14	38.50	11.20	1.25	9.25	11.00	11.36
3	38.20	38.14	11.00	1.25	7.36	9.25	11.18
4	38.44	38.20	10.82	1.25	5.70	7.35	10.96
5	39.60	38.44	10.80	1.21	3.70	5.70	11.00
6	40.86	39.60	10.80	1.18	1.70	3.70	11.00
7	42.20	40.86	10.80	1.12		1.70	10.96
8A	43.05	43.15	4.20	.43			
8B	43.15	42.20	6.50	.68			
9	42.78	43.05	10.80	1.12			
10	42.62	42.78		1.12			
11	42.52	42.62		1.14			
12	42.41	42.52					
13	42.20	42.41					
14		42.20					
15		42.20					
29	43.63	44.38	8.82	.94	9.25	11.00	9.34
30	41.73	43.63			7.35	9.25	9.22
31	42.38	41.73			5.70	7.35	9.06
32		42.38			3.70	5.70	9.04
33					1.70	3.70	9.03
34			14.50	1.57		1.70	14.70
35							
36							
37							
38							
39							
40							
41							
42							
43			19.53	2.00			
64	42.38	25.72	20.31	2.94			
65	21.52	25.72	14.96	2.41			
66	24.36	21.52	13.38	2.41			
67	30.71	24.36	11.34	1.57			
68	44.38	30.71	15.22	1.05			

Gore detail

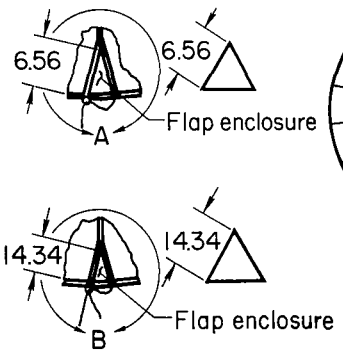

View K-K & L-L

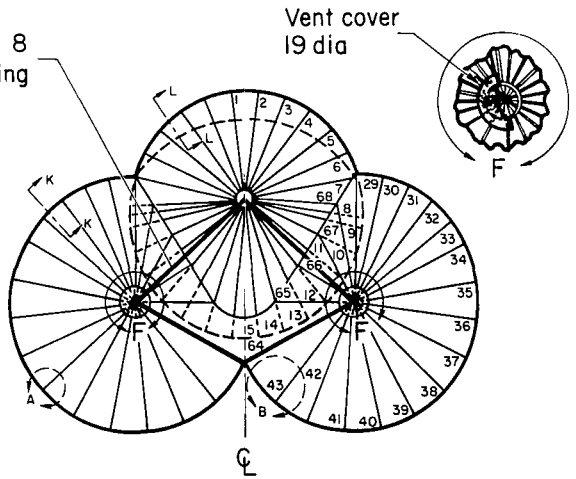

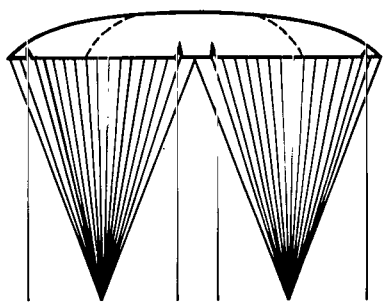

All dimensions in inches

Nominal diameter	12 ft
Nominal area	113 ft^2
Suspension line diam	.08 in.
Suspension line length	12 ft

Suspension lines to gores 38 through 42 and 45 through 49 grouped together for Δl_c control and lines to gores 7 through 23 grouped together for Δl_i control.

(f) Configurations 7 and 8.

Figure 2.- Continued.

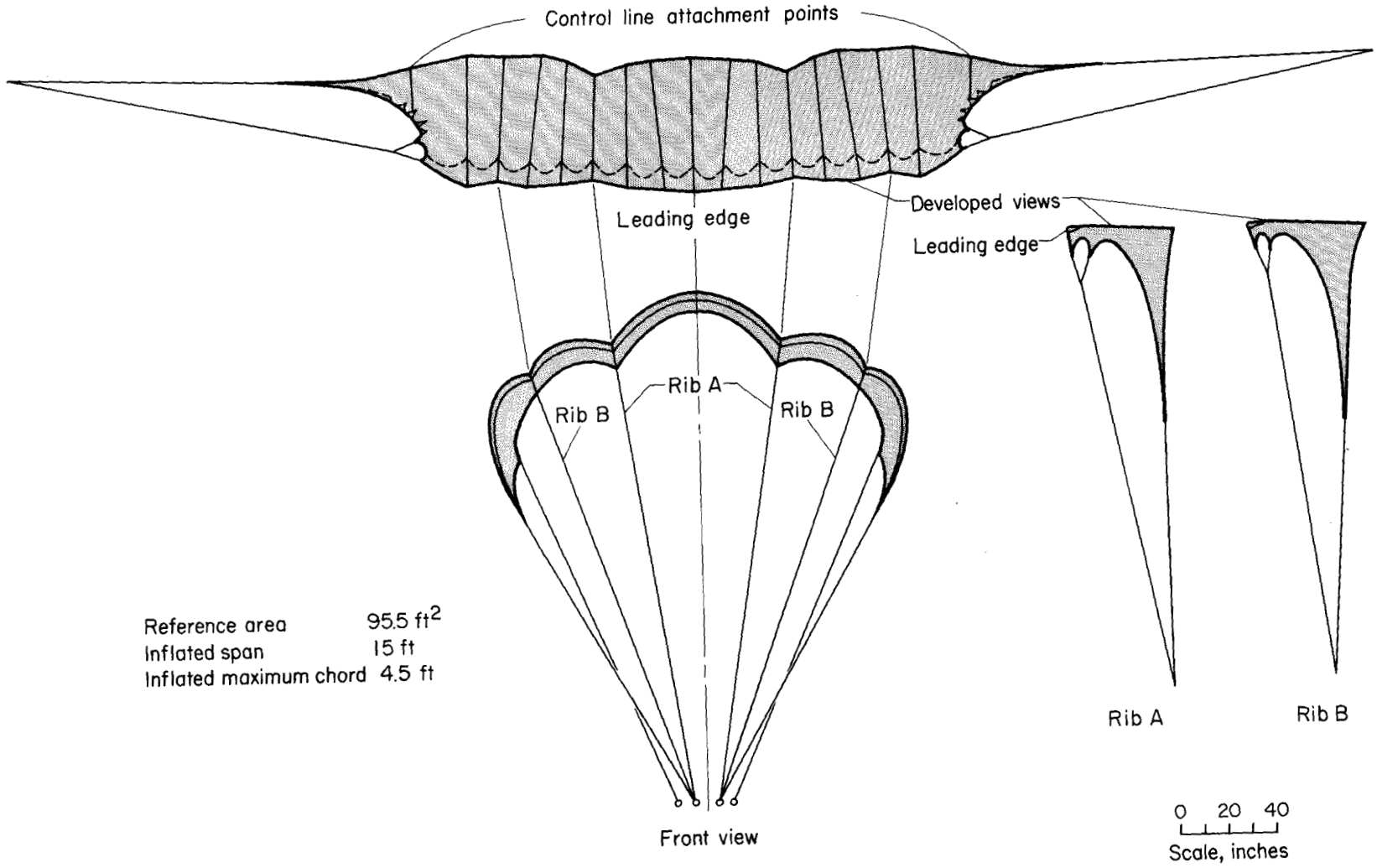

(g) Configuration 9.

Figure 2.- Continued.

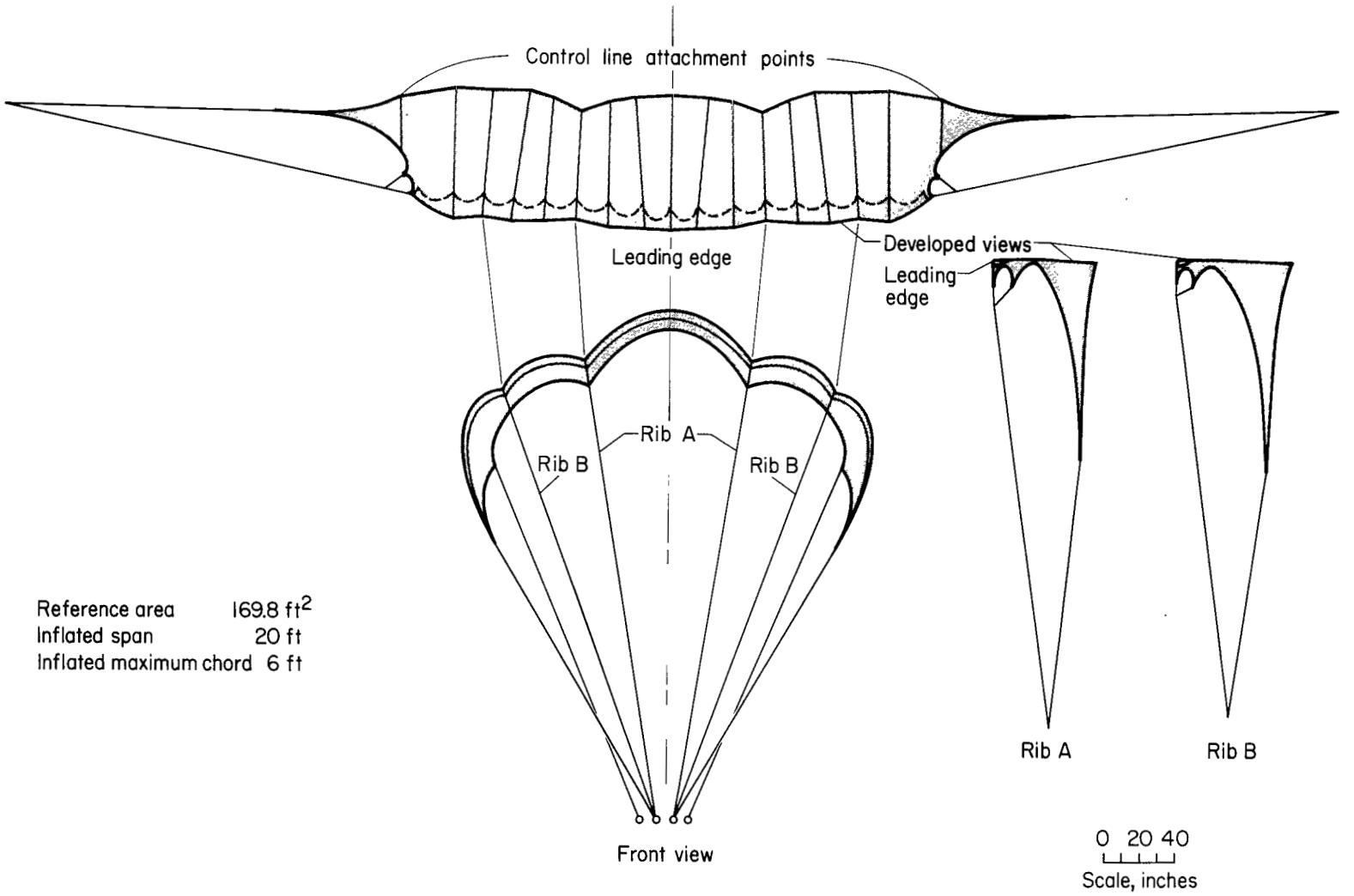

(h) Configuration 10.

Figure 2.- Continued.

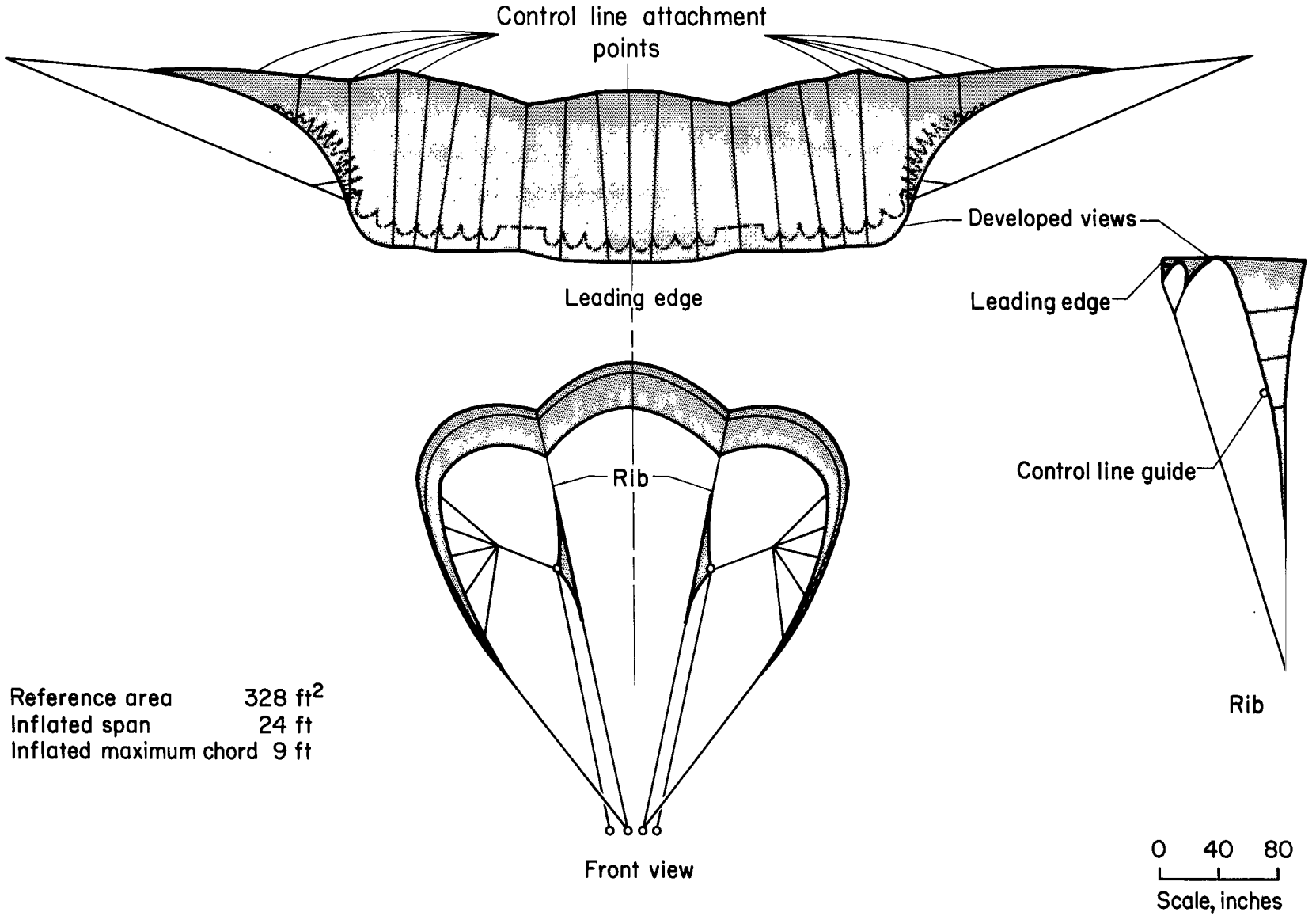

(i) Configuration 11.

Figure 2.- Concluded.

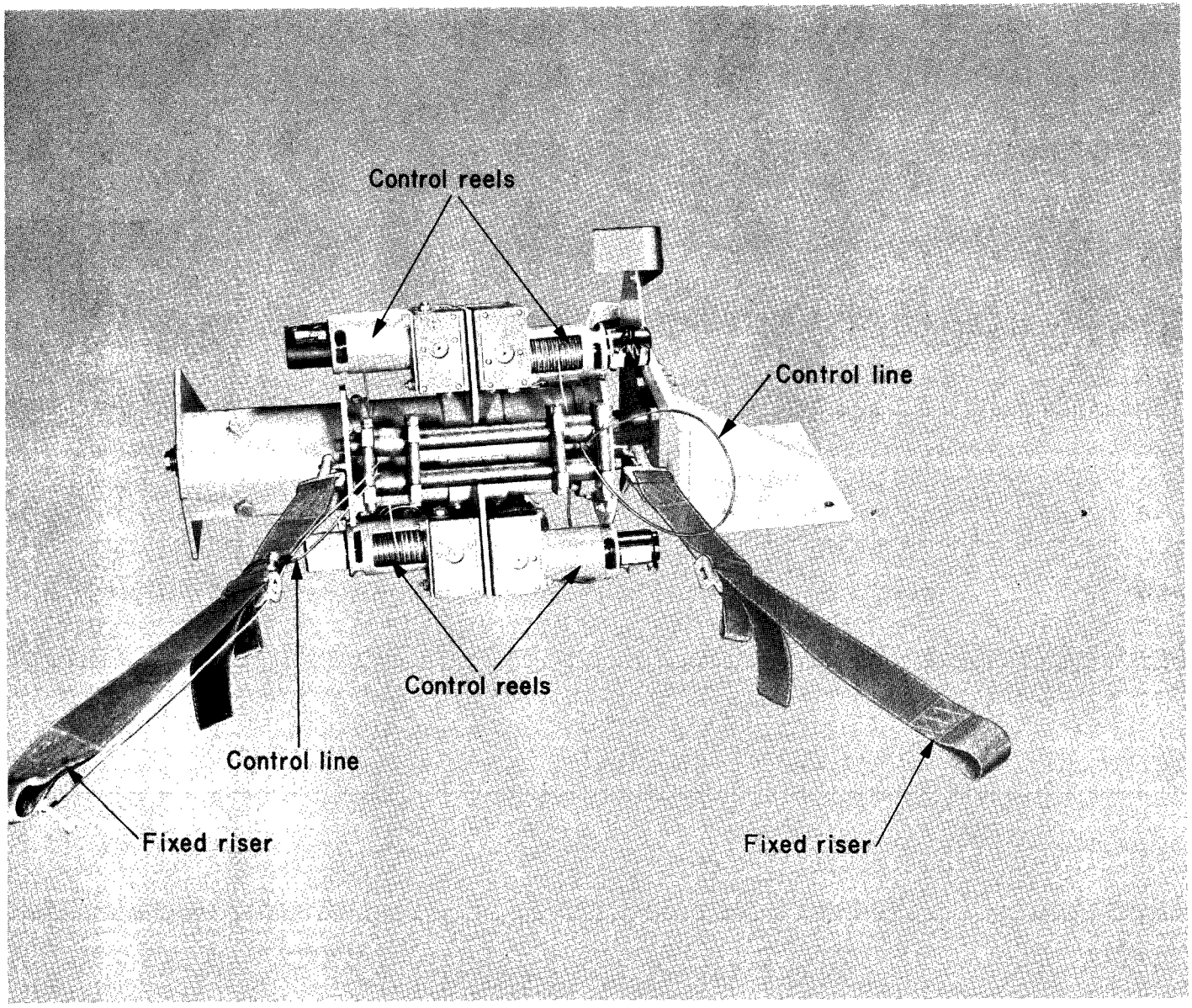

Figure 3.- Control mechanism.

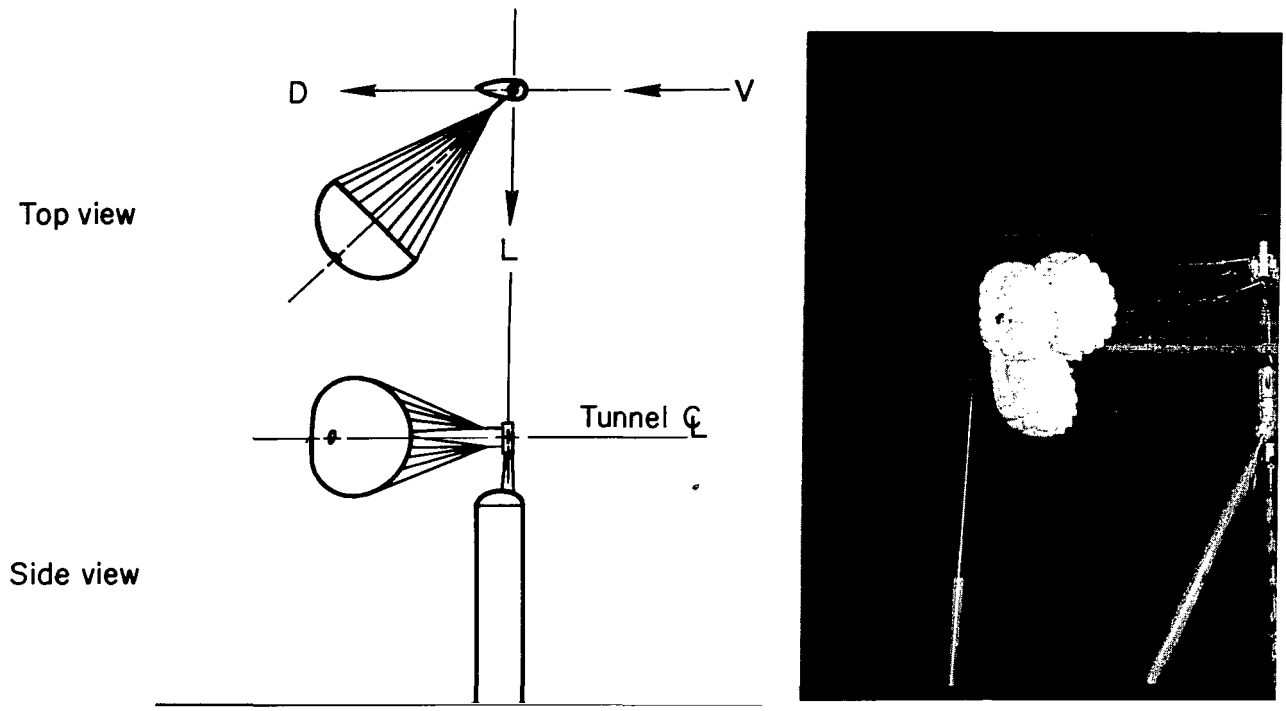

(a) Horizontal flight.

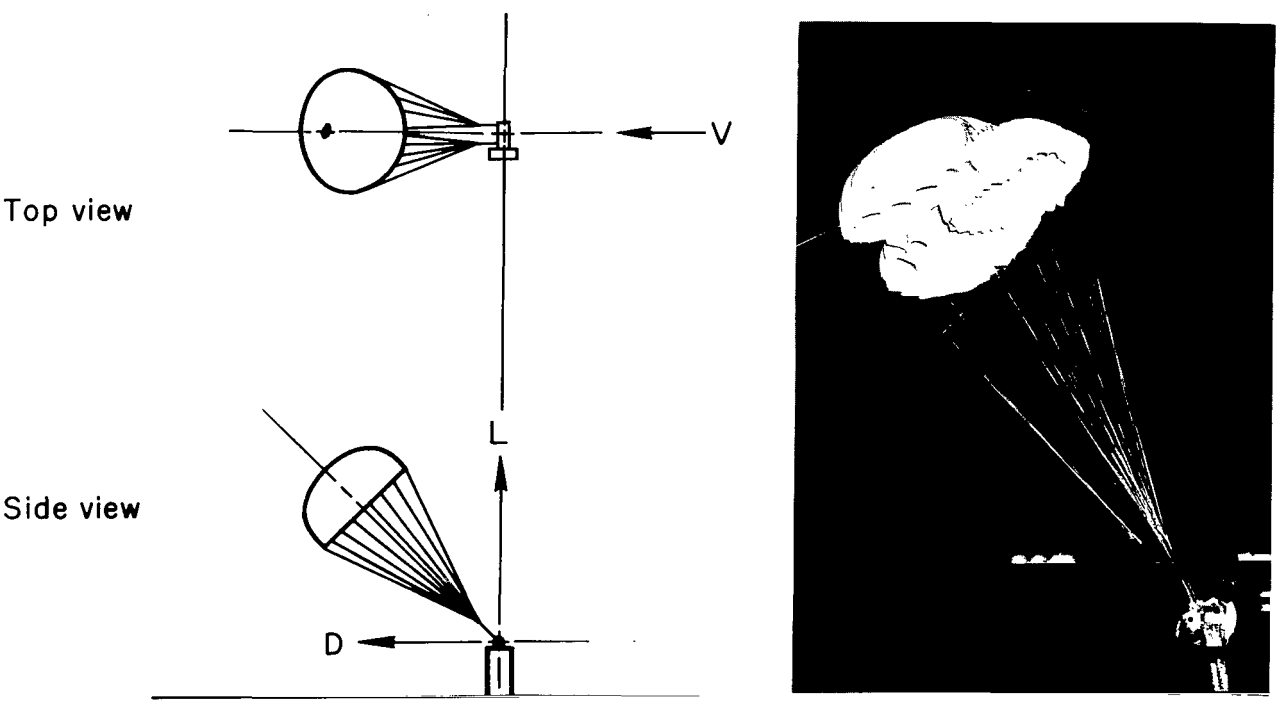

(b) Vertical flight.

Figure 4.- The two methods of mounting the parachutes in the wind tunnel.

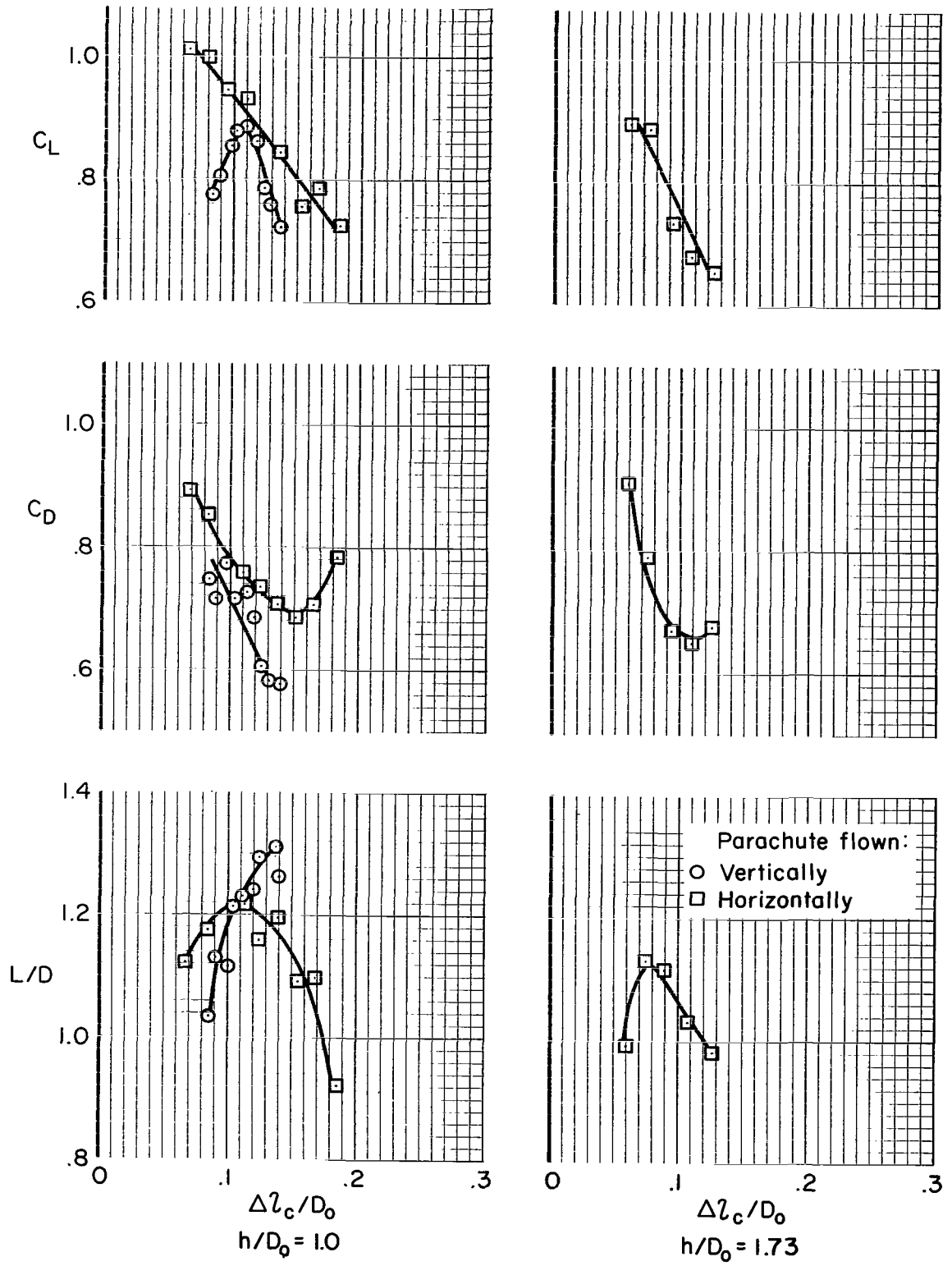

(a) Configuration 1, V = 30 fps.

Figure 5.- Aerodynamic characteristics of basic configurations.

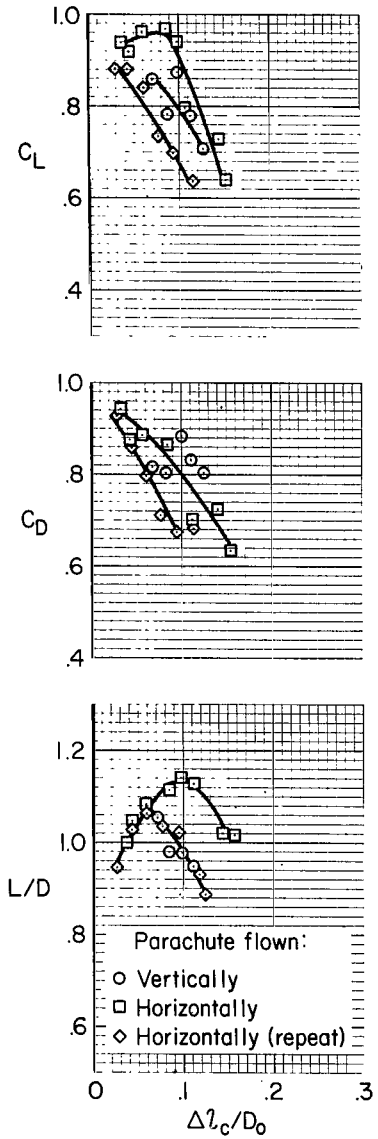

(b) Configuration 2; V = 30 fps, h/D_o = 1.0.

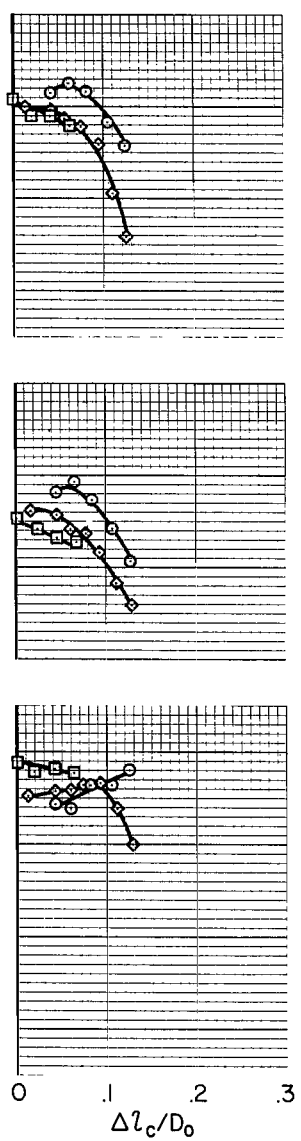

(c) Configuration 3; V = 30 fps, h/D_o = 1.0.

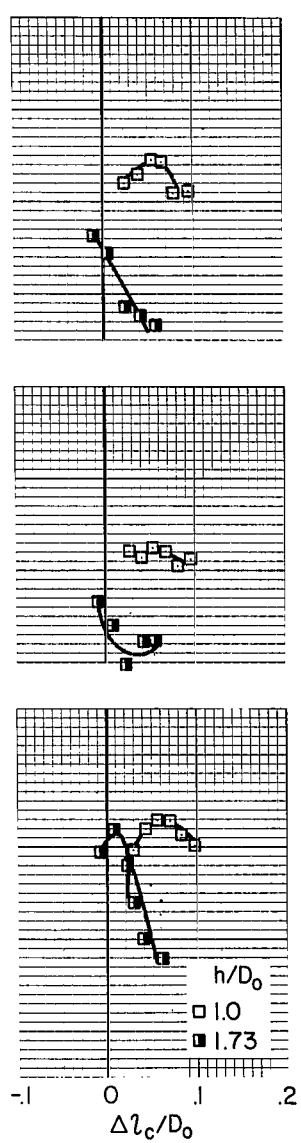

(d) Configuration 4; V = 30 fps, flown horizontally.

Figure 5.- Continued.

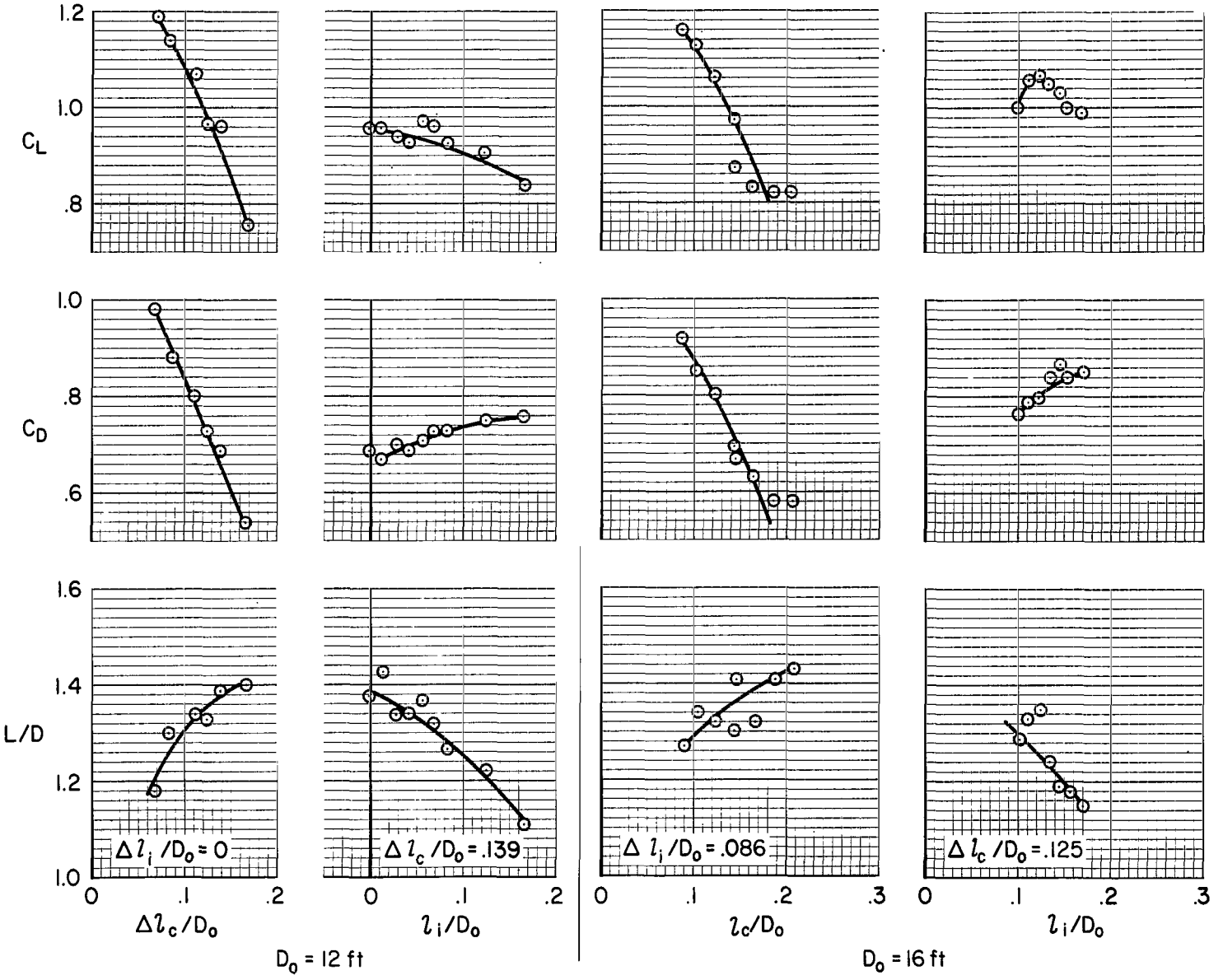

(e) Configuration 5; V = 30 fps, h/D_o = 1.0.

Figure 5.- Continued.

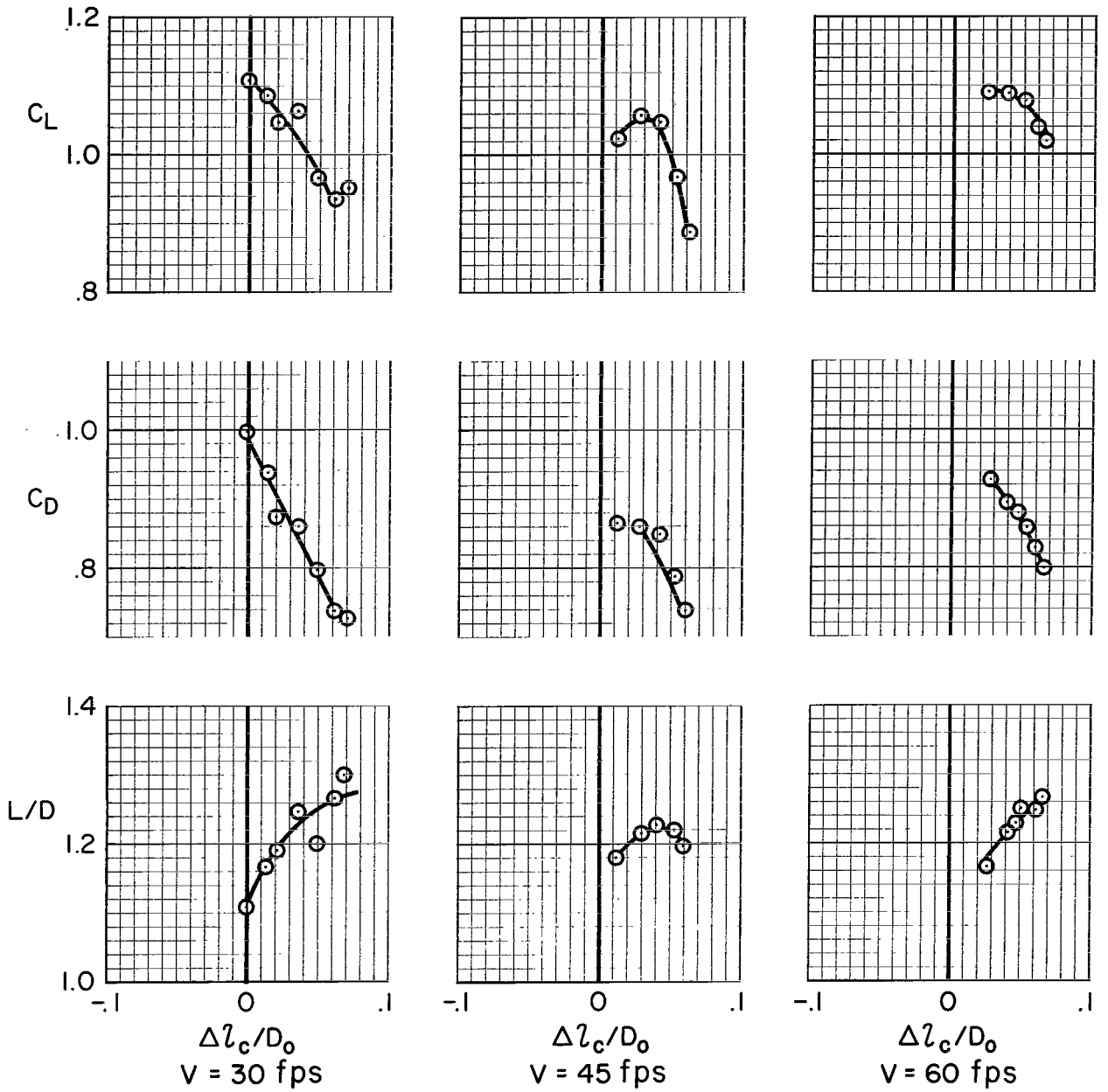

(f) Configuration 6, h/D_o = 1.0.

Figure 5.- Continued.

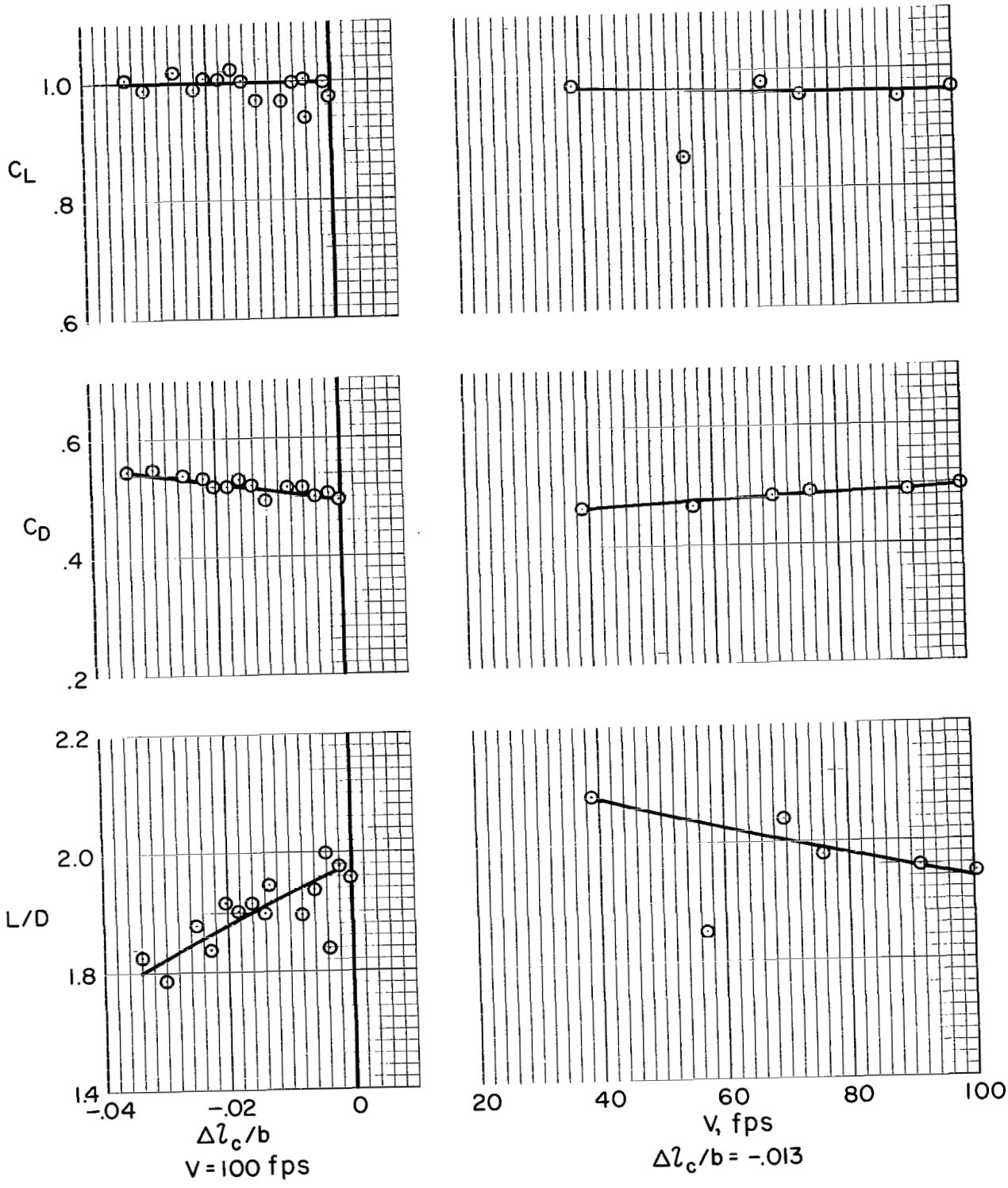

(g) Configuration 9.

Figure 5.- Continued.

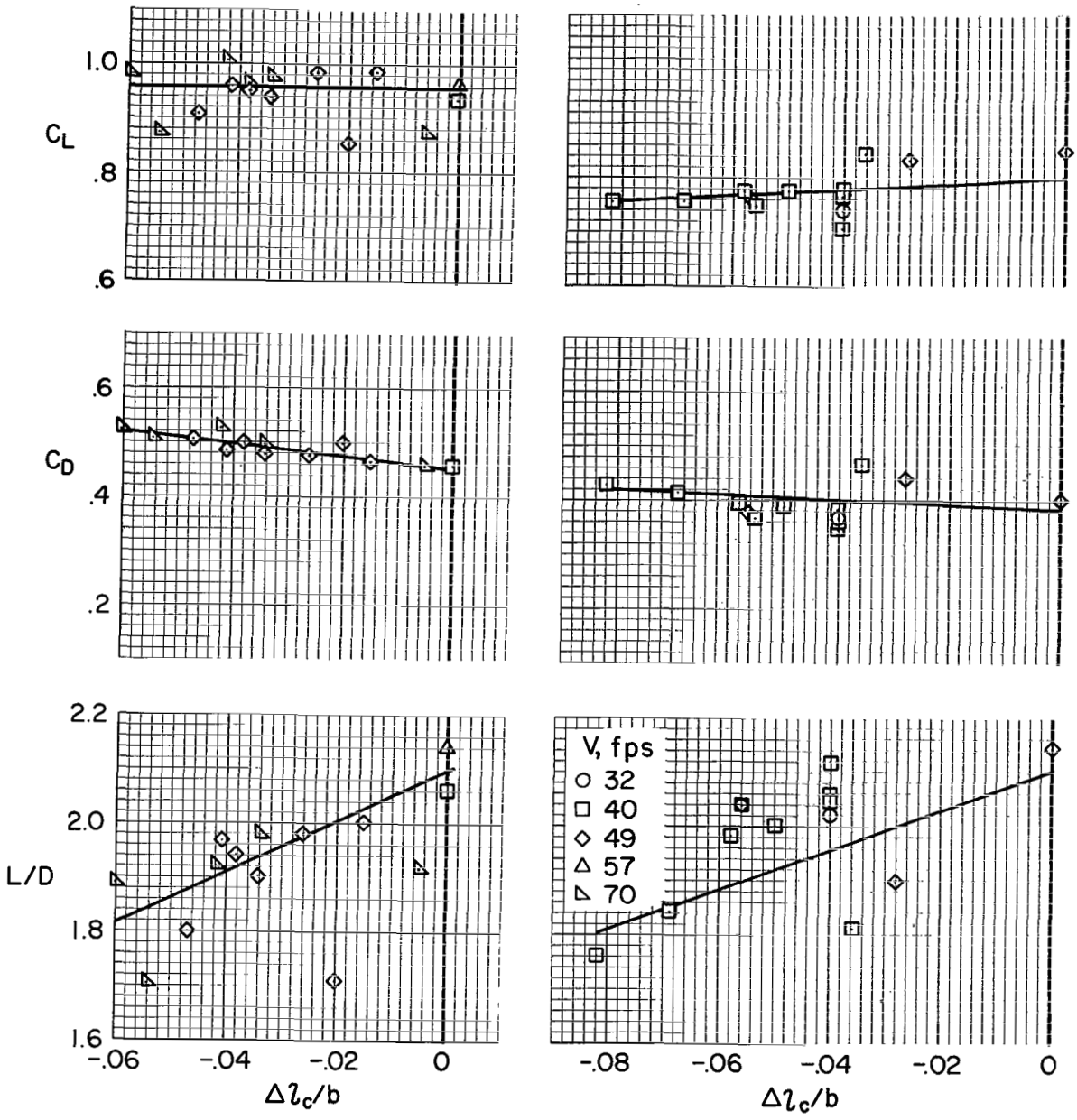

(h) Configuration 10.

(i) Configuration 11.

Figure 5.- Concluded.

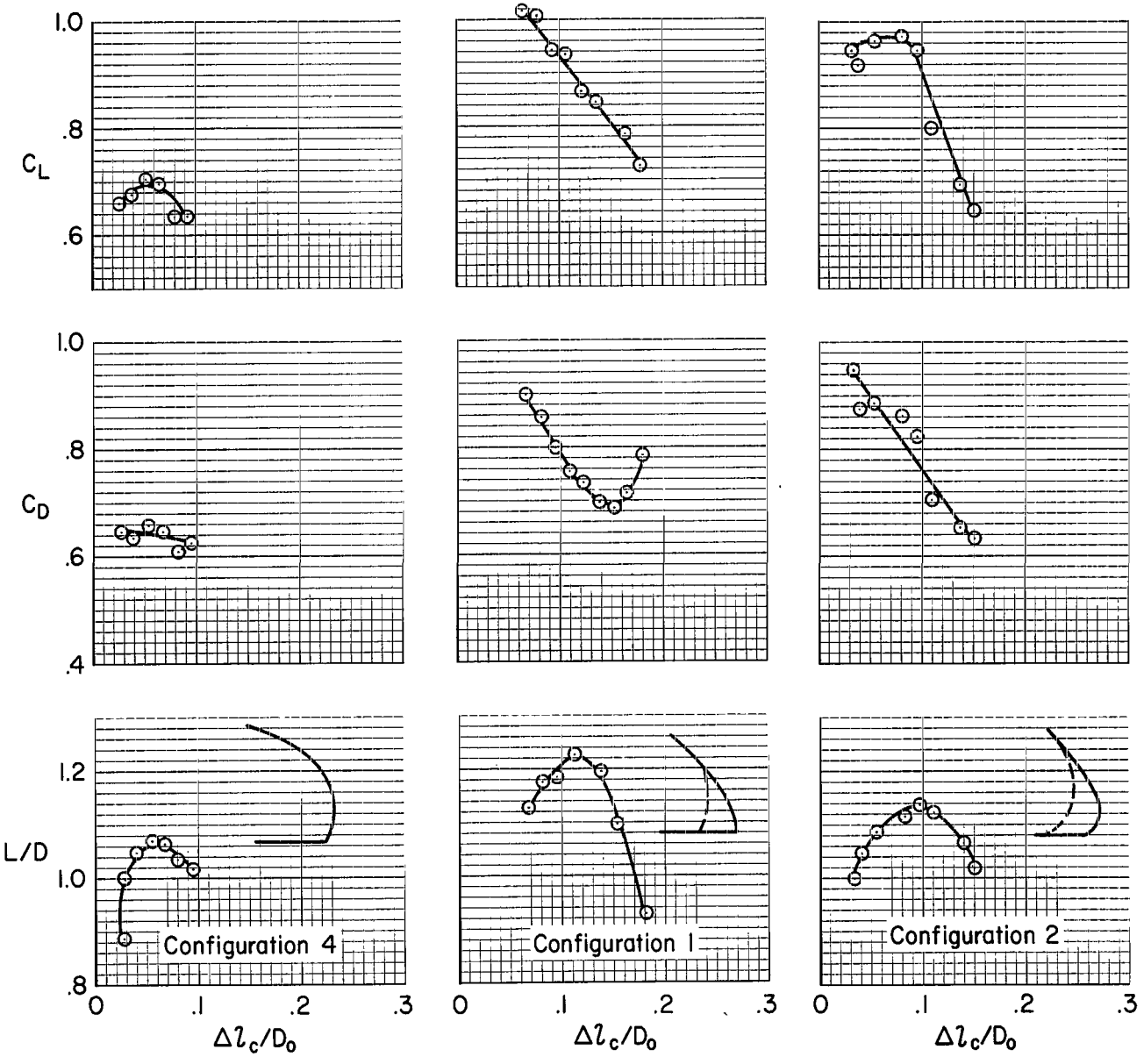

Figure 6.- Effect of leading-edge skirt extension; flown horizontally, $h/D_o = 1$, V = 30 fps.

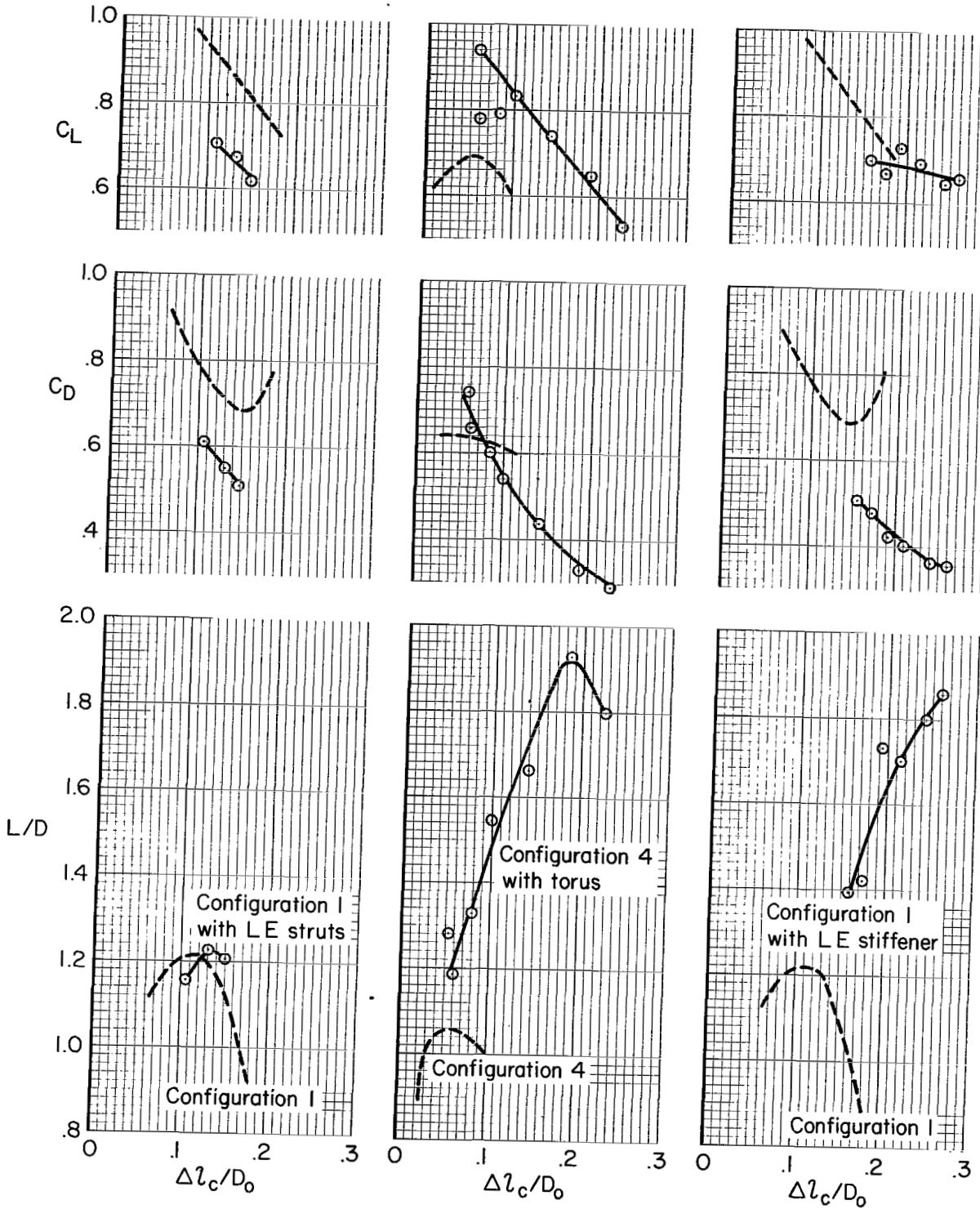

Figure 7.- Effect of canopy support devices; flown horizontally, $h/D_o = 1$, V = 30 fps.

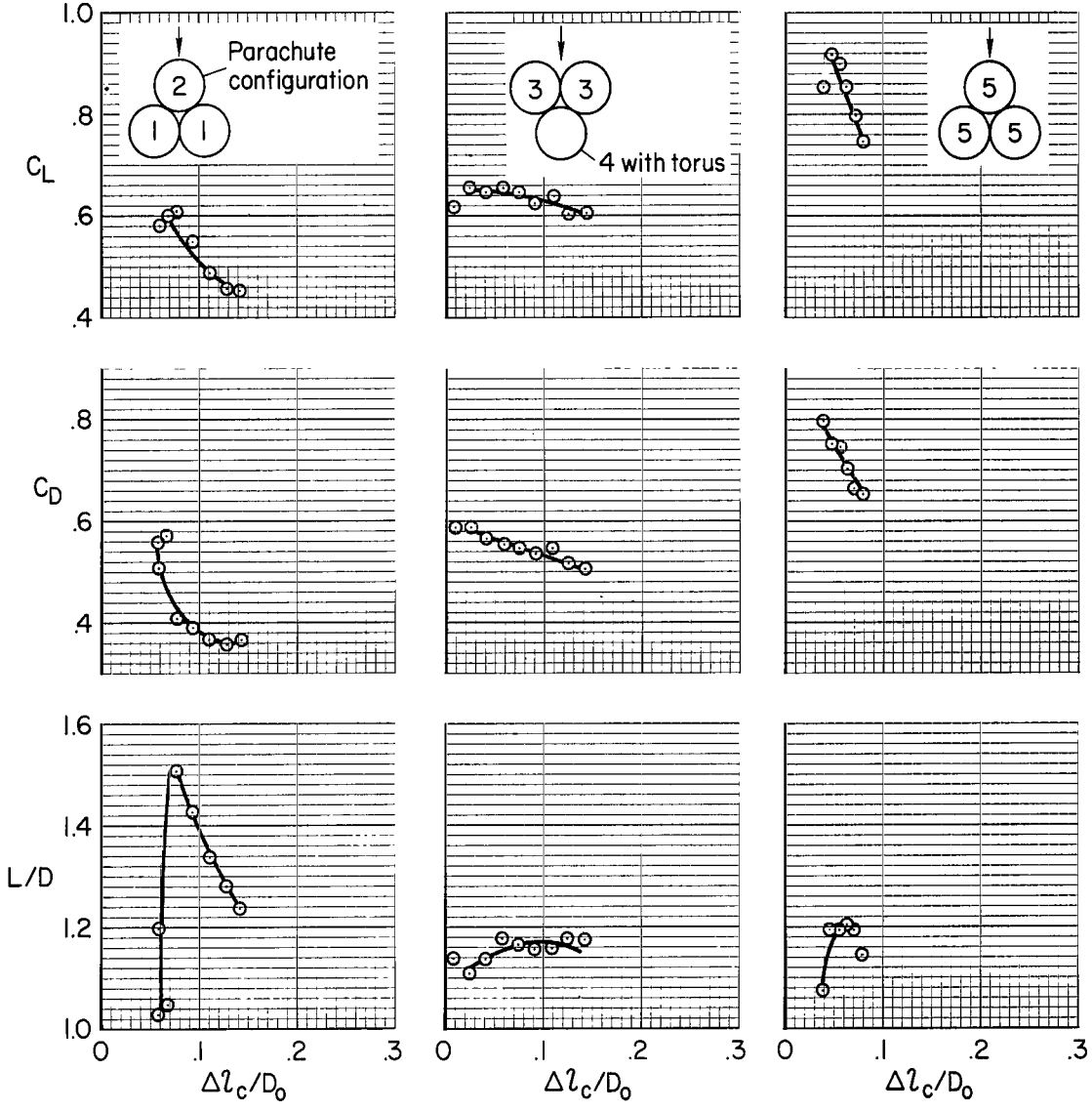

Figure 8.- Aerodynamic characteristics of clusters of parachutes; flown horizontally, $h/D_o = 1$, V = 30 fps.

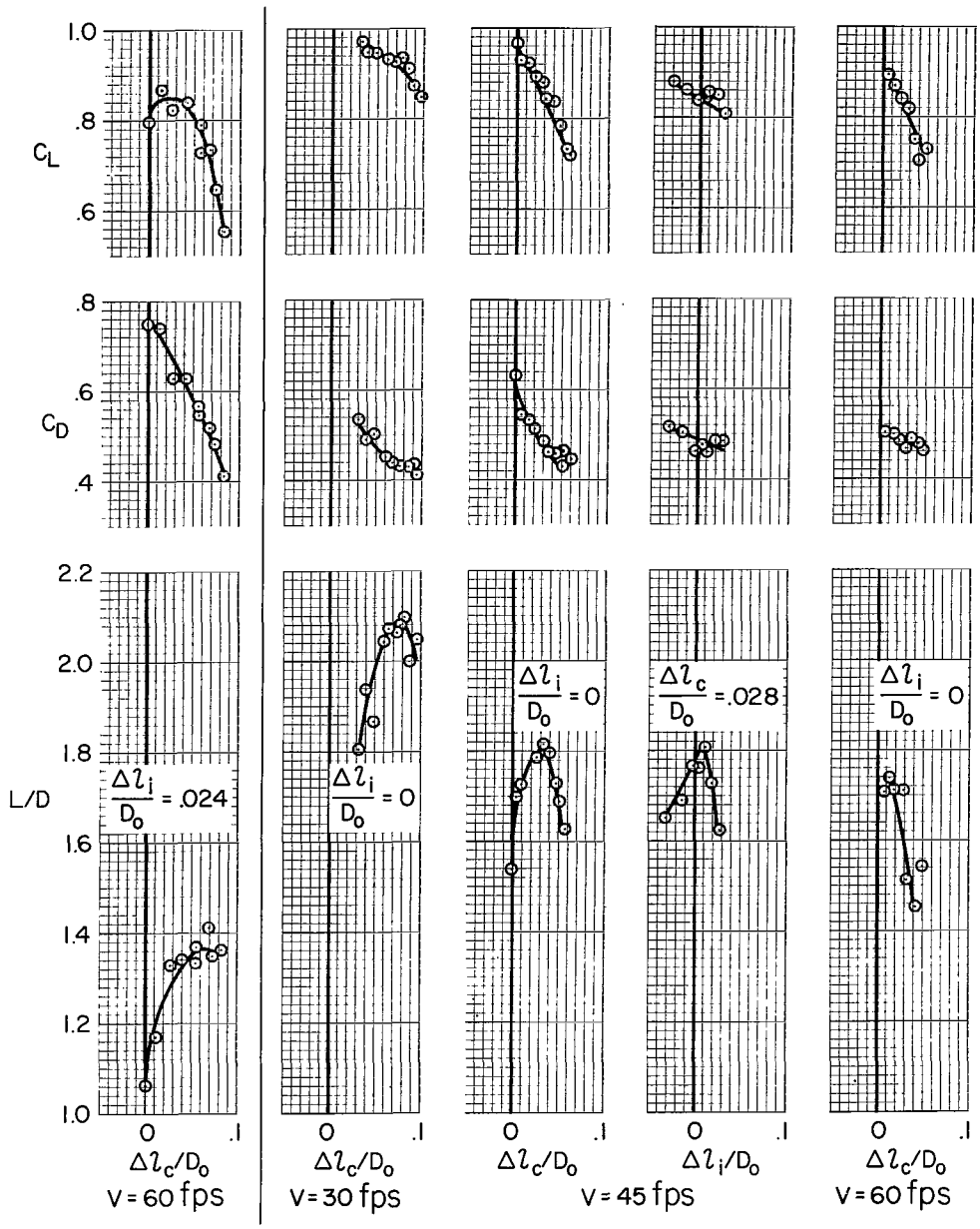

(a) Configuration 8.

(b) Configuration 7.

Figure 9.- Aerodynamic characteristics of shaped parachutes, $h/D_o = 1$.

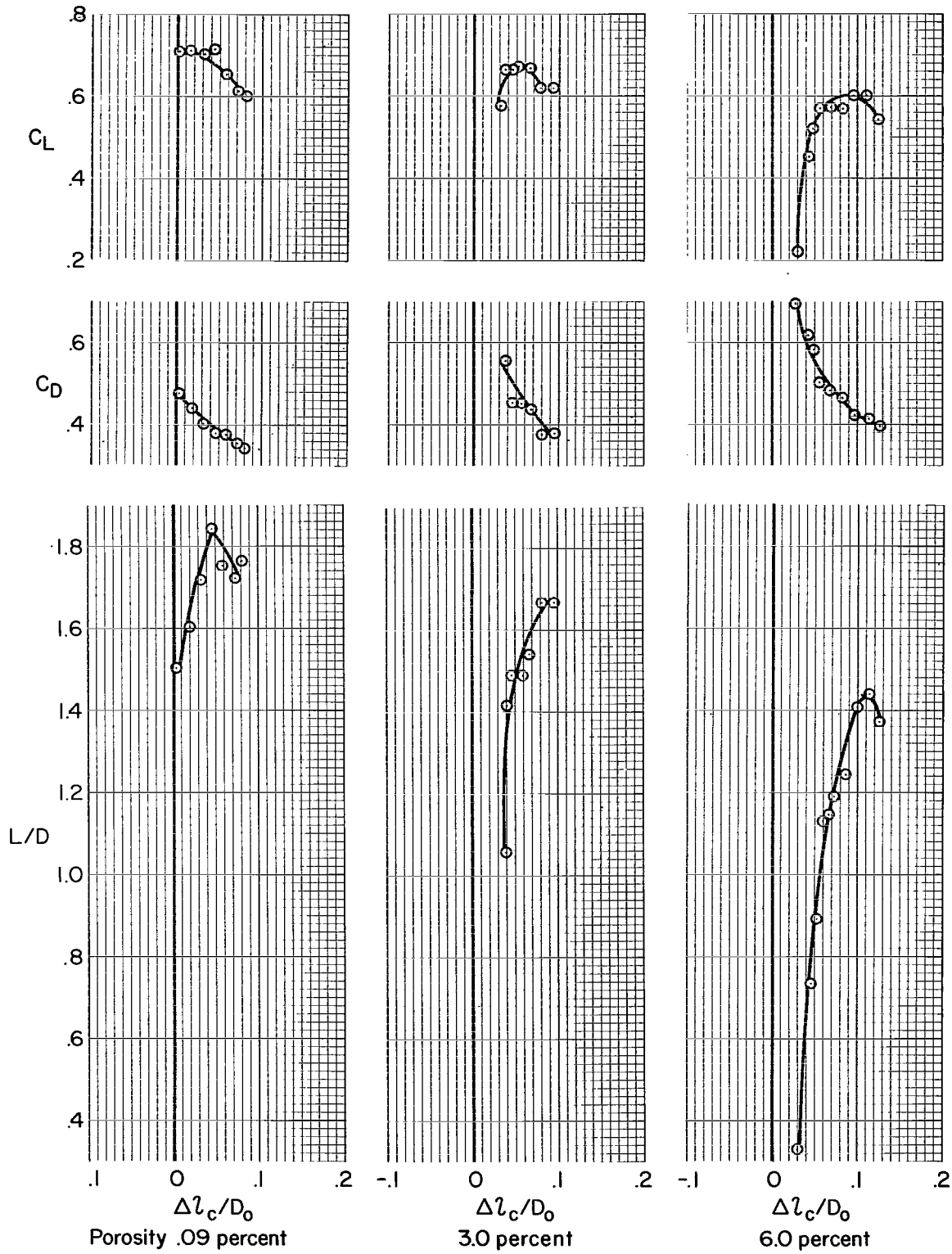

Figure 10.- Effect of porosity; configuration 7, V = 40 fps, $\frac{\Delta l_i}{D_o} = 0$.

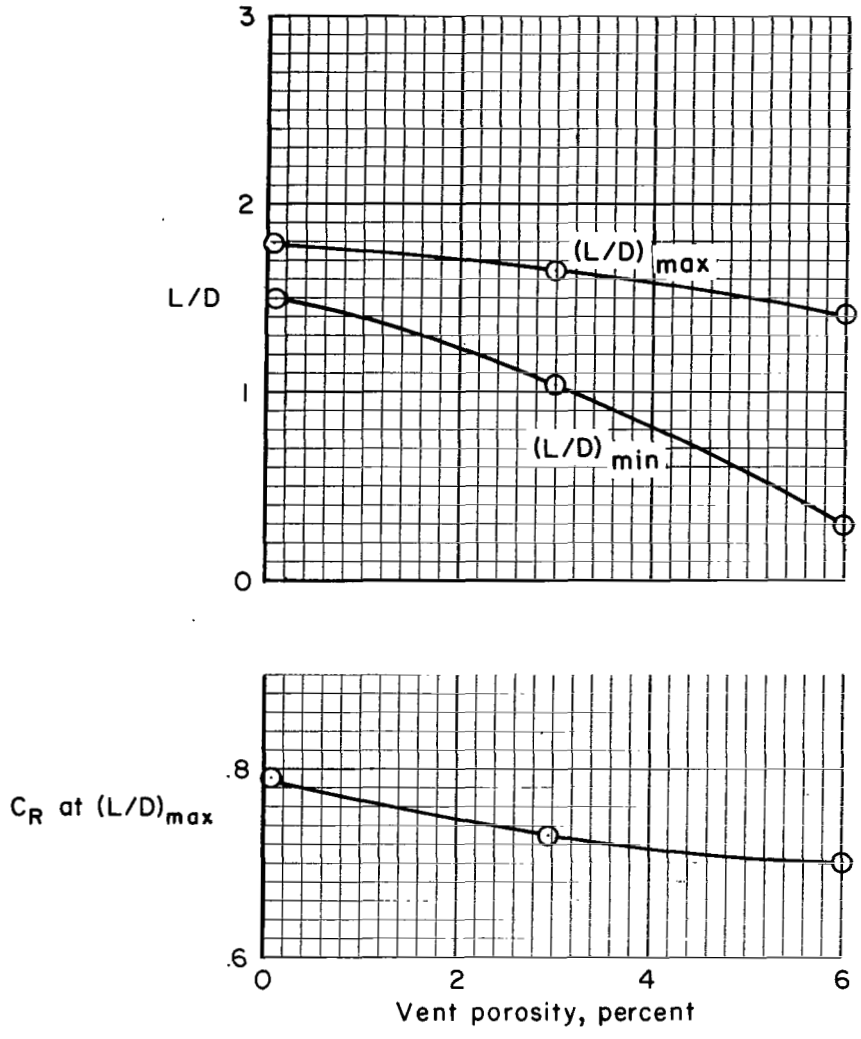

Figure 11.- Effect of porosity on glide capability; configuration 7, V = 40 fps.

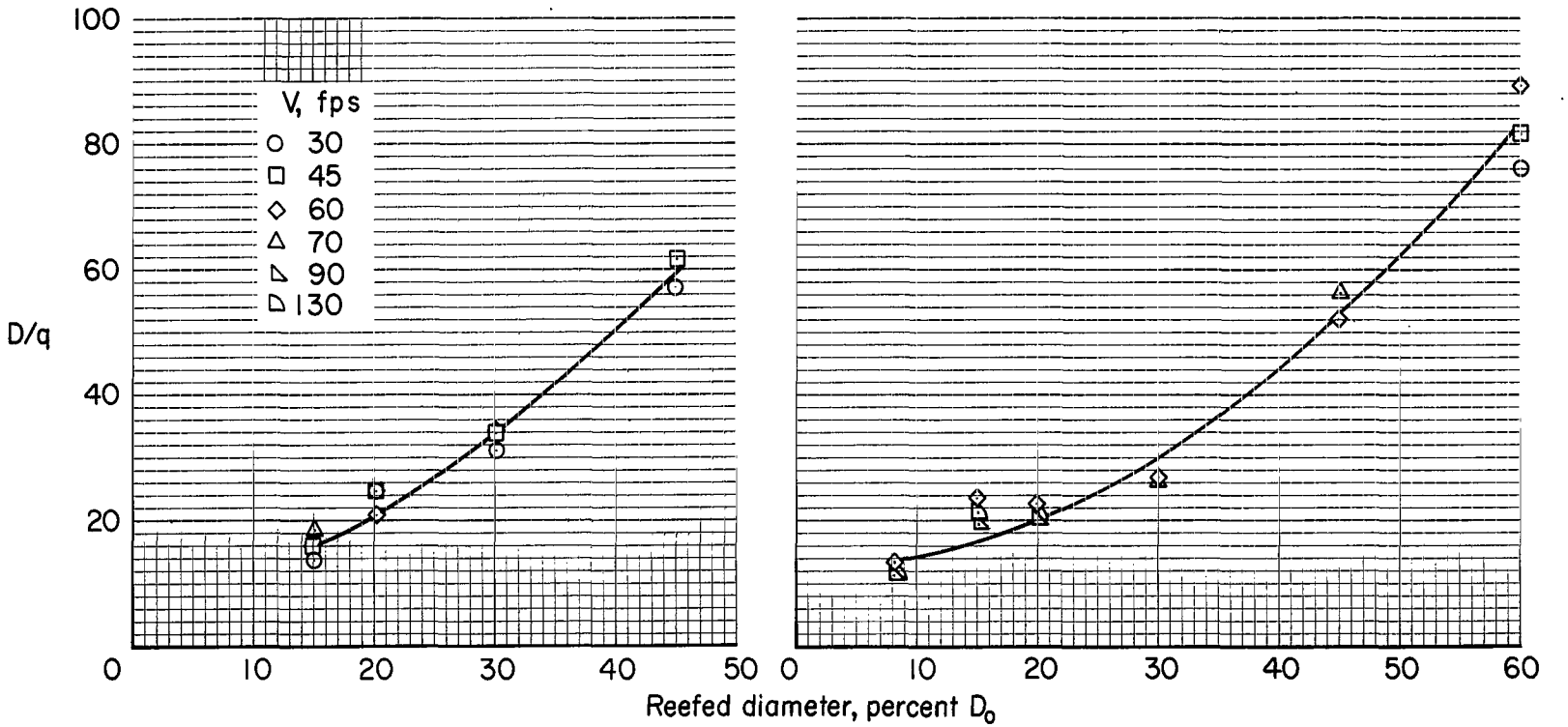

(a) Configuration 7.

(b) Configuration 5.

Figure 12.- Drag of reefed parachute.

"The aeronautical and space activities of the United States shall be conducted so as to contribute . . . to the expansion of human knowledge of phenomena in the atmosphere and space. The Administration shall provide for the widest practicable and appropriate dissemination of information concerning its activities and the results thereof."

—NATIONAL AERONAUTICS AND SPACE ACT OF 1958

NASA SCIENTIFIC AND TECHNICAL PUBLICATIONS

TECHNICAL REPORTS: Scientific and technical information considered important, complete, and a lasting contribution to existing knowledge.

TECHNICAL NOTES: Information less broad in scope but nevertheless of importance as a contribution to existing knowledge.

TECHNICAL MEMORANDUMS: Information receiving limited distribution because of preliminary data, security classification, or other reasons.

CONTRACTOR REPORTS: Scientific and technical information generated under a NASA contract or grant and considered an important contribution to existing knowledge.

TECHNICAL TRANSLATIONS: Information published in a foreign language considered to merit NASA distribution in English.

SPECIAL PUBLICATIONS: Information derived from or of value to NASA activities. Publications include conference proceedings, monographs, data compilations, handbooks, sourcebooks, and special bibliographies.

TECHNOLOGY UTILIZATION PUBLICATIONS: Information on technology used by NASA that may be of particular interest in commercial and other non-aerospace applications. Publications include Tech Briefs, Technology Utilization Reports and Notes, and Technology Surveys.

Details on the availability of these publications may be obtained from:

SCIENTIFIC AND TECHNICAL INFORMATION DIVISION

NATIONAL AERONAUTICS AND SPACE ADMINISTRATION

Washington, D.C. 20546